CHALMERS
UNIVERSITY OF TECHNOLOGY

# Quantifying the climate impact for future scenarios of Swedish aviation by developing a climate model

Master's thesis in Industrial Ecology

ERIC NYDÉN

DEPARTMENT OF SPACE, EARTH AND ENVIRONMENT

CHALMERS UNIVERSITY OF TECHNOLOGY
Gothenburg, Sweden 2022
www.chalmers.se

Master's thesis 2022

# Quantifying the climate impact for future scenarios of Swedish aviation by developing a climate model

ERIC NYDÉN


CHALMERS
UNIVERSITY OF TECHNOLOGY

Department of Space, Earth and Environment
*Physical Resource Theory*
Chalmers University of Technology
Gothenburg, Sweden 2022

Quantifying the climate impact for future scenarios of Swedish aviation by developing a climate model
ERIC NYDÉN



Supervisors: Anneli Kamb and Daniel Johansson
Examiner: Daniel Johansson

Master's Thesis 2022
Department of Space, Earth and Environment
Physical Resource Theory
Chalmers University of Technology
SE-412 96 Gothenburg
Telephone +46 31 772 1000

Cover: 'White airplane under the clouds' photo by Andreas Weiland @aweiland

Typeset in LaTeX
Printed by Chalmers Reproservice
Gothenburg, Sweden 2022

Quantifying the climate impact for future scenarios of Swedish aviation by developing a climate model

ERIC NYDÉN
Department of Space, Earth and Environment
Chalmers University of Technology

# Abstract

Emissions from global aviation contribute by a quantity of roughly 4-5% of the total anthropogenic climate forcing. Out of this forcing, contrail cirrus contributes to the largest direct warming effect of aviation-related emissions. The formation of contrail cirrus is dependent on the sooting propensity of jet fuel during fuel combustion. Emitted soot particles allow for ice crystals to form as water vapor condenses onto the particles, in turn establishing condensation trails under the right ambient conditions. Reducing soot emissions could as such prove to limit the climate warming of aviation substantially, one way of doing this is by the implementation of sustainable aviation fuels.

This thesis investigates the climate impact of different scenarios pertaining to the development of Swedish aviation and the use of sustainable aviation fuels up until 2050. This is done from the perspective of Swedish bunkering of jet fuel. By the development and application of a climate model, it is found that in the most optimistic scenario, a relative reduction of 46-53% in terms of the global surface temperature change contribution of Swedish aviation is possible in 2050. This is in comparison to a future development of aviation which follows historic trends. Additionally, it is also found that the application of sustainable aviation fuels proves to be more potent in terms of reducing the total warming effect of aviation, as opposed to reducing annual fuel use or maintaining a high yearly efficiency gain, during the investigated time period. The key reason for this is the reduction of contrail forcing due to sustainable aviation fuels, rather than the reduction in $CO_2$ emissions these fuels also lead to.

Keywords: aviation; bunkering; climate model; contrails; global warming; sustainable aviation fuel.

# Acknowledgements

Firstly, I would like to extend my gratitude towards my two supervisors, Anneli Kamb and Daniel Johansson, whose expertise and guidance made this work possible. I thank my friends for providing good company during my time of writing this thesis (and throughout). Also, a thank you goes out to my family, for misinterpreting me when trying to explain my thesis but smiling and being supportive nonetheless.

Eric Nydén, Gothenburg, June 2022

# List of Acronyms

Below is the list of the most common acronyms that have been used throughout this thesis listed in alphabetical order:

| | |
|---|---|
| ERF | Effective Radiative Forcing |
| HEFA | Hydroprocessed Esters and Fatty Acids |
| IPCC | Intergovernmental Panel on Climate Change |
| IRF | Impulse Response Function |
| SAF | Sustainable Aviation Fuel |

# Contents

# 1 | Introduction

## 1.1 Background

In the 6th and most recent assessment report by the IPCC, climate warming is shown to be increasing by the year and at a pace which makes reaching the 1.5°C goal of the Paris Agreement seem implausible. A future global climate in which the temperature rise stays below 2°C will require serious cutbacks when it comes to emissions, otherwise irreversible changes to the Earth's environment are to be expected (Mason-Delmotte et al. 2021).

Emissions from aircraft contributes a substantial amount to the global warming of the planet - global aviation accounts for approximately 4-5% of the total anthropogenic climate forcing [1] (Lee et al. 2021). The combustion of jet fuel releases gases such as carbon dioxide ($CO_2$), nitrogen oxides ($NO_x$) and water vapour ($H_2O$) into the atmosphere and between 2013 and 2018 aviation induced $CO_2$ emissions has seen an annual increase of 5% per year. In the short term however, the most potent climate forcer stems from the condensation trails left behind by the aircrafts. With the potential of forming miles wide cloud-like cirrus which traps outgoing radiation within the Earth system, the yearly radiative effect of condensation trails surpasses that of the other aviation related emissions. A recent study by Lee et al. (2021) suggests that contrail cirrus contributed to a global effect of 57.4 $mWm^{-2}$ in 2018, with $CO_2$ being the second largest contributor with an effect of 34.3 $mWm^{-2}$.

Wealthy countries are the main contributors; per capita Sweden ranks as 7th in the world when it comes to aviation related emissions (SOU 2022). Emissions are commonly attributed according to one of two perspectives. Either to aircraft which are fueled within a country, known as bunkering, or to the travel done by countries' inhabitants. In recent years the Swedish passenger count has been increasing at a yearly rate of 5%, with domestic flights seeing a stagnation at the same time as international flight volumes have been growing. Both nationwide and international measures have been adapted in Sweden to reduce the climate impact associated with aviation. Air taxation was implemented in 2018 and plans to make domestic air travel fossil free by 2030 have been put in place by the Swedish aviation industry (Kamb and Larsson 2019). International flights are regulated by the market-based instrument CORSIA (Carbon Offsetting and Reduction Scheme for

[1] Throughout the thesis climate forcing refers to the concept of effective radiative forcing, which is different to radiative forcing. The distinction is further explained in the theoretical background.

International Aviation) which is managed by The International Civil Aviation Organization (ICAO). Any growth in $CO_2$ emissions post 2020 has to be compensated by the airlines through purchasing emission units, however CORSIA does not account for other aviation related emissions outside of $CO_2$. Similarly Swedish aviation is part of the EU Emissions Trading System (EU ETS) where emissions are regulated by having to buy rights to pollute.

An increasingly relevant alternative to reduce emissions is through the use of sustainable aviation fuels (SAF). However, because of the cost of SAF the industry is not incentivized to introduce these fuels as a tool to reduce emissions directly, even though they are applicable in the emissions trading systems (SOU 2019). A reduction obligation quota (sv. Reduktionsplikt) was introduced in Sweden in 2021, which enforces the use of sustainable aviation fuels in order to decrease the amount of greenhouse gas emissions from fossil based jet fuel in the aviation industry. SAF encompasses fuels which are derived from renewable biomass sources or is produced synthetically. Every year, jet fuel providers will have to reduce emissions associated with aviation fuel by incorporating an increasing share of SAF blended with the fossil jet fuel. The required reduction in emissions started at 0.8% in 2021 and is set to gradually increase each year, ultimately ending at 27% 2030. In addition to the reduced $CO_2$ emissions from cutback of fossil fuels, recently produced research suggests that the use of SAF also reduces the formation of condensation trails (Voigt et al. 2021; Bräuer et al. 2021; Kärcher 2018; Burkhardt et al. 2018).

Research relating to the use of SAF and it's potential impact of the radiative balance of the atmosphere and on the climate impact is scarce. The climate effect of SAF-combustion during flight conditions is limited and research is still ongoing within the area. The results of the 100% SAF flight tests of the VOLCAN and ECLIF3 projects are being projected to come out later in 2022 (Sampson 2021; Airbus 2021). Klöwer et al. (2021) and Grewe et al. (2021) have looked at aviation's contribution to global warming, including future scenarios of zero-carbon fuels, however no study of this kind has been done at a national level in Sweden. Understanding the effectiveness of SAF, as a method to reducing emissions from aviation, is important for implementing policies to enforce the use of it in the aviation industry but also to understand the rate necessary in order to accomplish set out climate targets.

## 1.2 Purpose and problem definition

The purpose of this thesis is to investigate and quantify the climate impact of Swedish aviation both historically and for future scenarios of air travel and use of sustainable aviation fuels.

To accomplish this, 12 scenarios describing potential outcomes for the future of Swedish aviation up until the year 2050 will be put together and analysed. A climate model accounting for aviation related emissions will be developed in the programming language Python in order to evaluate each scenario and the climate impact associated with them. Specifically, the model will through several steps be

capable of computing the rise in global surface temperature based on the formation of condensation trails, emissions of $CO_2$ as well as carbon feedback mechanisms. Furthermore, this will include the need to establish a simple relationship between blending ratios of SAF and the change in effective radiative forcing which the change in fuel composition facilitates. As such, a small-scale literature study on research of sustainable jet fuels will be conducted as to determine the climate relevant properties of SAF.

By investigating potential future scenarios the thesis will aim to answer the following questions:

- What contribution to global warming can be attributed to bunkering of Swedish jet fuel?
- What is the potential of sustainable aviation fuels and the reduction obligation quota, from a climate impact perspective?
- What appears to be the most potent strategy for reducing the climate impact of end-of-pipe aviation emissions?

## 1.3 Limitations

Combustion of jet fuel emits several gases which interacts with the atmosphere and its composition in different ways, thus having to be modeled according to separate chemical and microphysical procedures (Lee et al. 2021). The focus of this thesis will be on modelling the two largest aviation induced climate forcers; condensation trails and $CO_2$, and will as such not include the lesser warming effects of $NO_x$ and $H_2O$ or cooling effects of sulfate aerosols.

In regards to jet fuels, emissions are not treated from a life cycle perspective, meaning that the emissions associated with producing jet fuels are not accounted for in the overall climate impact. Current regulations allow jet fuel blends consisting of a maximum of 50% SAF (SOU 2022), in this thesis it is assumed that technological advancements will allow for fuel blends made up of over 50% SAF by 2035, stretching to 100% by 2045.

Swedish emissions will be attributed according to Swedish bunkering of jet fuel, meaning fuel which is fueled within Sweden. This effectively illustrates the potential of policy decisions in Sweden and is relevant from the point of view in that local fueling practices can be governed. On the flip side it can be argued that countries such as The Netherlands, which serves a big part of traffic for connection routes at Schiphol airport, is attributed to a disproportionate amount of emissions (SOU 2019).

Lastly, the global COVID-19 pandemic has drastically reduced flight volumes, as an effect of major travel restrictions. On average, 2020 saw a reduction of 45% in total flights (Klöwer et al. 2021). It is non-trivial to project the recovery of the aviation industry after this event and the lasting consequences. This thesis will not address nuances regarding COVID-19's potential effect in regards to the recovery period of

the industry, but instead assume a linear recovery to previous flight volumes as in 2019 pre-pandemic, by the end of 2025.

# 2 | Theoretical background

## 2.1 Climate forcing & feedback

Climate forcers denotes different factors which stimulate climate change. Generally the change is caused by a shift in the energy flux of the Earth's climate system, this could be by reflecting and absorbing incoming shortwave solar radiation or by trapping outgoing longwave radiation within the Earth system. Additionally, feedback response from climate change itself can lead to further shifts in the flow of energy, e.g. through cloud formation or outgassing of carbon. As such climate forcers can be both anthropogenic and natural and include greenhouse gases, volcanic ash and solar radiation in itself.

Energy flux is often measured in watts per square meter ($Wm^{-2}$) and can be either positive or negative, in turn defining a warming or cooling effect on the climate. The quantification of the energy flux, called the radiative forcing (RF), is measured as the energy flux at the top of the atmosphere. The concept is used to evaluate the impact different forcers have on the climate, including from both natural and anthropogenic sources. A link between the RF and the change in temperature can be established by a linear relationship based on a climate sensitivity parameter (Forster et al. 2021). Commonly, an alteration of the concept, effective radiative forcing (ERF), is used since it considers fast feedback mechanisms of the climate, in turn leading to a better linear relationship with the subsequent temperature response (Faber et al. 2022; Smith et al. 2021). In practice, what differs between the concepts is the use of an efficacy parameter which determines an individual climate sensitivity, dependent on the investigated forcer. The concept of efficacy better accounts for the impact of forcers that aren't homogeneously distributed (Lee et al. 2021), such as condensation trails. In turn, this results in a large difference between the quantified RF and ERF for condensation trails. The efficacy $r_i$ of a given forcer is multiplied by the climate sensitivity of $CO_2$; $\lambda_i = r_i \lambda_{CO_2}$. The efficacy of $CO_2$ is always given as $r = 1$ and for the case of contrails $r < 1$ (Lee et al. 2021).

Changes in energy flux are furthermore assumed to be both additive and linear. The response to shifts in the global energy flux is a change in the steady state of the global temperature. In a steady state there is a balance between incoming and outgoing radiation, but additional incoming radiation causes an energy imbalance, in turn shifting the equilibrium through a rise in temperature (Forster et al. 2021).

## 2.2 Modelling of aircraft emissions

The way in which the climate system reacts to different climate forcers and feedbacks can be approximated through modelling of climate response systems. Sausen and Schumann (2000) state that the most accurate estimations of the climate impact of aviation-related emissions can be obtained with a comprehensive atmosphere-ocean general circulation model, which is paired together with a carbon cycle model as well as a model for atmospheric chemistry. These comprehensive models are computationally demanding but can be emulated efficiently by linear response models. The climate systems can be described as dynamic systems, where the linear response function describes the response to a perturbation which disturbs the equilibrium state of the system according to Equation 2.1. The response $x(t)$ depends on past perturbations $f(\tau)$ which are weighted by the response function $g(t-\tau)$.

$$x(t) = \int_{-\infty}^{t} f(\tau)g(t-\tau)\ d\tau + ... \tag{2.1}$$

The response function varies depending on the given climate forcer. This because of factors such as the associated lifetime, atmospheric distribution, effect on energy flows and more, all affects their respective climate impact differently (Joos et al. 2013). For instance, the change in atmospheric $CO_2$ concentration is dependent on carbon sinks in the terrestrial system as well as in the ocean, all relating to the Earth's carbon cycle. In addition, the change in $CO_2$ induced forcing is approximately logarithmically dependent on the current atmospheric $CO_2$ concentration and thus previous emissions (Joos et al. 2013). On the other hand, the temperature response to an energy imbalance is dependent on the oceans capability to absorb and store heat (Xie and Vallis 2012) and as such it has to be modeled by a different response function.

## 2.3 Formation of contrail cirrus

The combustion of aviation fuel at cold temperatures can lead to the formation of condensation trails, often referred to as contrails. Contrails are formed as an effect of emitted water vapour and soot particles from the aircraft exhaust. Under the right conditions the emitted water vapour, as well as the ambient water vapor, condenses onto the soot particles. The surrounding air cools the droplets, freezing them to ice, in turn leaving a contrail behind the aircraft (Voigt et al. 2021; Bräuer et al. 2021). The lifetime of these contrails are highly variable. Whether or not contrails form, dissipate or persist and remain in the atmosphere is affected by the atmospheric temperature, pressure, ambient humidity and the composition of the aircraft emissions (Schumann 1996). These circumstances make up to two underlying atmospheric conditions that have to hold for persistent contrails to form (Gierens et al. 2020). Namely the Schmidt-Appleman criterion, which describes the conditions under which contrails are formed. The criterion thermodynamically relates contrail formation to the change in relative humidity, as emitted water vapor comes into contact with the surrounding air (Schumann 2005; Gierens et al. 2020).

And secondly, that the surrounding air has to be in an ice supersaturated state, meaning that the relative humidity in relation to the amount of ice must be higher than 100% for contrails to be persistent, and not dissipate within minutes after their formation (Gierens et al. 2020). The cold circumstances required for these conditions generally occur at altitudes of 8-13 km (Kärcher 2018).

Persistent contrails can develop into contrail cirrus, which resembles ordinary cirrus clouds. During the time in which contrail cirrus remains in the atmosphere, it affects the radiative balance in two ways (Voigt et al. 2021). Firstly, it has a cooling effect on the Earth by reflecting incoming solar radiation back into space, and secondly it has a warming effect by reflecting outgoing infrared radiation back towards the Earth. By adding the two effects it is found that contrails cirrus causes a net positive radiative forcing, in turn increasing the surface temperature on the Earth.

The number of ice crystals and their size is the determining factor in how contrail cirrus interacts with radiation. Fewer and larger ice crystals sublimate and sediment faster (Voigt et al. 2021) and also decreases the optical depth of the contrails, thus reducing their albedo (Burkhardt et al. 2018). The number of ice crystals that form is dependent on the number of soot particles emitted, Kärcher (2018) estimates this relationship to be linear for current emissions which is in the range of $10^{14}$ to $10^{15}$ soot particles per kg fuel. Some loss of initial ice crystals is expected due to the vortex phase as seen in Figure 2.1. During this phase adiabatic heating causes sublimation of ice crystals within the vortex system. The fraction of ice crystals which sustain through the vortex phase is greatly variable (Unterstrasser 2016). Burkhardt et al. (2018) state that this loss is expected to be around 10% to 20% in relation to initial ice crystal numbers, depending on the ambient climate. The overall effect the number of ice crystals has on the radiative forcing is seen to be nonlinear. A halving of current ice crystal numbers would reduce the radiative forcing of contrails by 21%, whereas a 90% reduction of ice crystal numbers would decrease the radiative forcing with up to 69% (Burkhardt et al. 2018).

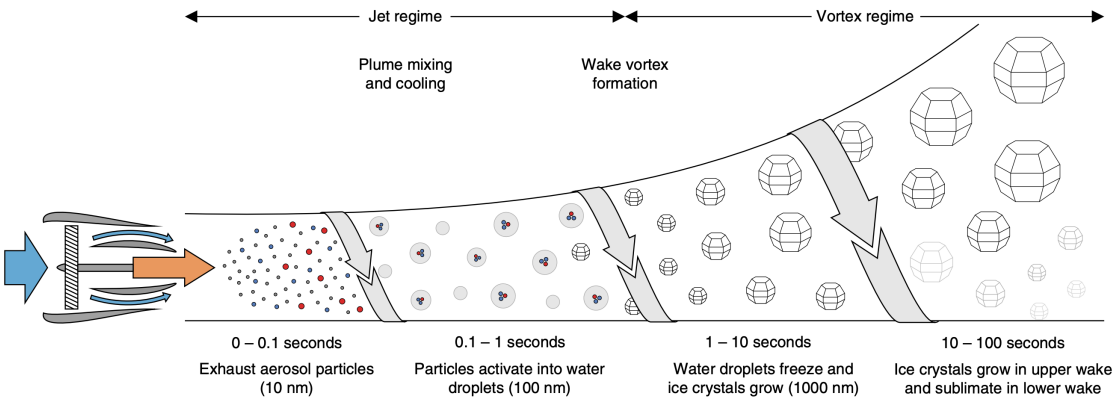


**Figure 2.1:** The timescale for which ice particles form after particle emissions from the aircraft exhaust. *Source:* Kärcher (2018) (CC BY 4.0).

## 2.4 Aviation fuel

Today's commercial aviation fuel is mainly made up of two different types of jet fuel; Jet A and Jet A1. Both jet fuels consist of kerosene, a fossil fuel which is derived from crude oil. The properties and structure of Jet A and Jet A1 are largely similar. The primary difference lies in the freezing point of the fuels, Jet A1 can withstand colder temperatures and is therefore used for flight routes operating under colder climate conditions (Air bp n.d.).

### 2.4.1 Fuel composition & characteristics

Kerosene-based jet fuels consist of a wide variety of hydrocarbons which are mixed to fulfill the physiochemical properties required of the jet engine specifications and ambient weather conditions. This includes having a high energy density, thermal stability and flash point, as well as having a low freezing point and enough lubricity for the engines to function well (Holladay et al. 2020). The hydrocarbons may differ in terms of molecular structure but they remain members of one of four chemical groups present in jet fuel; cyclo-alkanes, n-alkanes, iso-alkanes and aromatics (Faber et al. 2022).

Out of the hydrocarbons, the aromatics are found to be directly related to the sooting propensity of jet fuel. The hydrogen to carbon ratio decreases for fuels with a higher aromatic content, which in turn is found to increase the formation of soot particles in the aircraft gas turbines upon fuel combustion (Richter et al. 2021). Research suggests that one aromatic compound in particular, naphthalene, has a considerable effect on soot emissions (Faber et al. 2022; Bräuer et al. 2021). The aromatic content of commercial jet fuel varies and on average lies in the of span of 15 to 20%, with global standards allowing an upper limit of 25%. A lower limit of minimum 8% aromatics is required by the industry due to safety precautions, this because a lower aromatic content could lead to swelling of sealings within the fuel systems of the aircrafts. It is possible to reduce the aromatic content of conventional jet fuel through hydrotreatment, however there are no incentives to do so as it would also increase fuel costs (Faber et al. 2022).

### 2.4.2 Sustainable aviation fuel

Sustainable aviation fuel is an umbrella term for jet fuels produced from renewable or sustainable resources. They can be synthetically created (e.g. by the Fischer-Tropsch process) or be made from bio-based feedstocks. Synthesized fuel is created from a number of chemical processes and is typically derived from renewable hydrogen and carbon (Faber et al. 2022). Bio-based fuels can be derived from a number of different renewable sources such as camelina, lignin, rapeseed, jatropha and algae (Kandaramath Hari et al. 2015). SAF can be mixed with kerosene jet fuel to create more sustainable fuel blends. Mixing of the fuel types requires that the chemical structures of both fuels are the same, SAFs compatible for fuel blending are often referred to as drop-in fuels. According to current standards blending of up to 50%

SAF in respect to kerosene jet fuel is permitted (SOU 2019).

At the present Bio-SPK and FT-SPK are the two commercially available SAFs that are in use (Jiménez-Díaz et al. 2017). Both fuels types are Synthethic Paraffinic Kerosenes (SPK) and are compatible for blending with current jet fuels. Bio-SPK is commonly made from bio-derived oil which is synthesized to jet fuel through a number of different processes, including transesterification and hydroprocessing. One such fuel is HEFA-SPK (Hydroprocessed Esters and Fatty Acids). FT-SPK (Fischer-Tropsch), on the other hand is made from biomass which first is converted to gas, through a thermochemical process. Additional fuel conversion pathways includes converting alcohols to fuel or fermenting/catalytically upgrading sugars (Jiménez-Díaz et al. 2017), the development stage of the different fuels varies. Figure 2.2 displays the 'readiness' of different SAFs.

The advantage of drop-in fuel is twofold, it reduces the emitted $CO_2$ upon fuel combustion and also reduces the aromatic content of the mixed jet fuel, since SAF does not have any aromatic content (Faber et al. 2022). Reducing the aromatic content and thus the amount of soot particles being emitted then decreases the amount of particles for emitted water vapor to condense onto. As such it reduces ice crystal numbers and the overall radiative effect of condensation trails (Voigt et al. 2021).

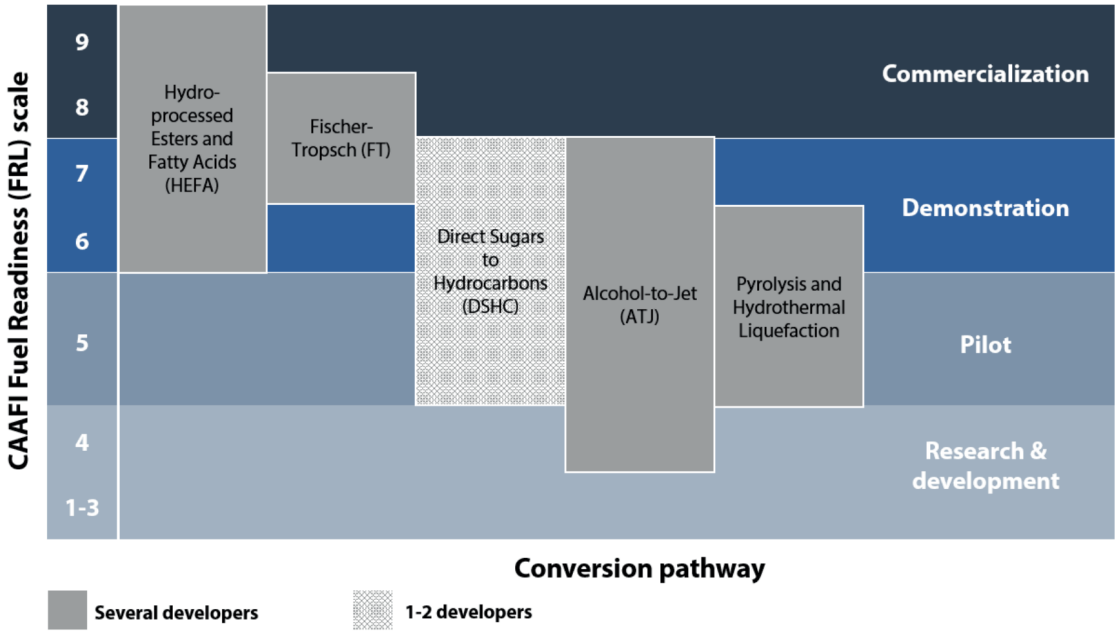


**Figure 2.2:** The development stage of different sustainable aviation fuels and the number of developers associated with eat fuel pathway *Source:* De Jong (2018).

# 3 | Methodology

## 3.1 Climate model

A climate model was developed in order to calculate the climate impact of the most significant aviation related emissions. Changes in the radiative balance were calculated for $CO_2$ emissions, contrail cirrus formation as well as carbon cycle feedback caused by the contrail induced temperature response. Both $CO_2$ emissions and carbon cycle feedback forcings were computed using a carbon cycle model. Contrail forcings were modeled linearly after the amount of yearly $CO_2$ emissions and based on the aromatic content of scenario-specific jet fuel. The computed radiative flux was then applied to an energy balance model to estimate the change in global surface temperature caused by the aggregated climate forcers. $CO_2$ emissions were treated as annual emissions pulses and were based on the fuel usage of bunkered fuel in Sweden. All fossil-based fuel was assumed to be of the Jet A1 type, for which a respective emission index was used. Jet A1 was used as the reference fuel both historically and for the non-SAF share of future scenarios.

The climate model was implemented in the programming language Python. The model is split up into several modules, each module having a specific task in calculating the overall climate impact according to the steps mentioned above. An abstraction of the logical structure of the model and the modules is depicted in Figure 3.1 where the program code associated with the model is delimited by the dashed border. The functionality of each module is described in further detail in the following sub-chapters. The input to the model was based on scenario-specific data spanning from 1973 to 2050 and included annual $CO_2$ emissions as well as the percent share of biofuels used in the Swedish aviation industry for each year. The construction of the scenarios is detailed further in Chapter 4.

The validity and accuracy of the model was tested and compared to research results of a study done by Lee et al. (2021), in which the impact on climate forcing from global aviation was investigated. The comparison was done by gathering historic $CO_2$ emissions from global aviation and using this data as input to the climate model. Emission data was taken from the supplementary material of Lee et al. (2021) for the time period of 1990-2018, and from Sausen and Schumann (2000), for 1940-1990.

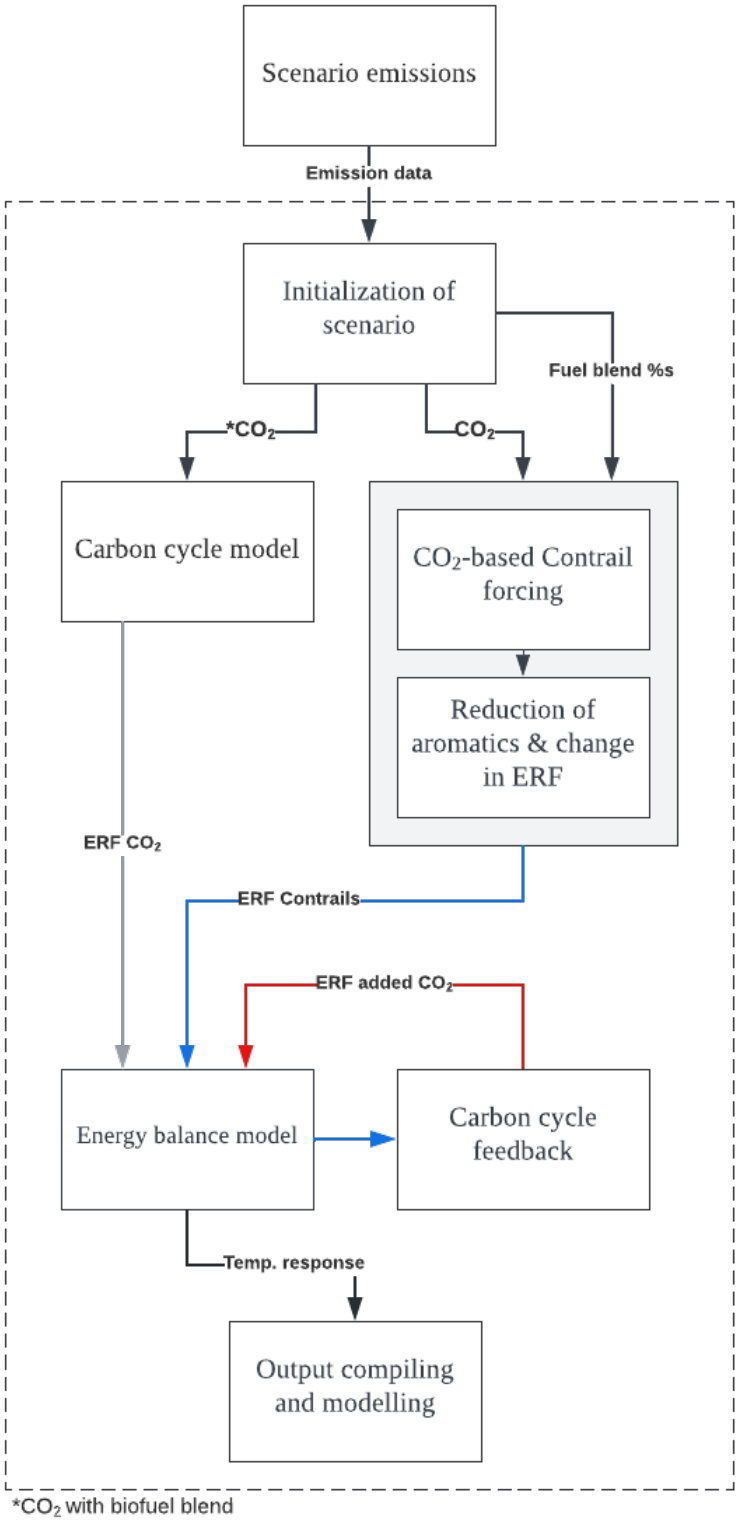


**Figure 3.1:** The climate model conceptualised within the dashed border, with associated modules and data dependency between modules.

### 3.1.1 Carbon cycle model

The carbon cycle model was divided into three steps, with the overall purpose to obtain the added effective radiative forcing from an emission of $CO_2$. The first step constituted calculating the change in the amount of $CO_2$ in the atmosphere, due to a $CO_2$ emission. This is referred to as the atmospheric $CO_2$ stock. The second step was compromised of computing how the perturbation of the atmospheric stock affects the $CO_2$ concentration of the atmosphere. Lastly, from the added concentration it was possible to quantify the additional ERF which the $CO_2$ emission gives rise to. In the model, the emissions were quantified as Tg $CO_2$ and were compounded as an annual emission for each year.

In order to obtain how the atmospheric stock of $CO_2$ changes based on an emission, different global carbon sinks have to be accounted for. These are what makes up the Earth's global carbon cycle. From a system analysis point of view, the carbon cycle can be described as a linear time-invariant system, where a $CO_2$ emission is treated as an input to the system, often referred to as an input signal. The input signal was modeled as a unit impulse (Dirac delta distribution), as described in Equation 3.1. The unit impulse is equal to zero at all points except at 0, where the quantified size of the emission impulse is expressed as $e_0$. For the case of this study, the unit impulse represents a singular impulse emission pertaining to a years worth of $CO_2$ emissions. Running the input signal through the system in turn produces an output signal which portrays the response of the system, i.e. the given change in atmospheric $CO_2$ stock due to a $CO_2$ emission.

$$e(t) = e_0\delta(t) \tag{3.1}$$

The dynamics of the carbon cycle system and how it responds to a unit impulse is described by its impulse response function (IRF), commonly this is known as the transfer function when applied to the Laplace transform. Describing the IRF of a system can be done by Green's function (Gasser et al. 2017). The IRF of the carbon cycle which was used in this study was of the same form as the one presented and used by Joos et al. (2013) and can be seen in Equation 3.2. The IRF is based on simulations of the Bern carbon cycle model, which is a model that exists in multiple variations and is often applied in climate research, including the climate investigations done by the IPCC. The IRF is constructed of multiple exponential functions which in turn describes the response to an atmospheric perturbation of $CO_2$, given by the sum of these exponentially decaying functions. The decaying functions represent different $CO_2$ sinks over different time scales, since the sinks operate over different time spans. In the IRF, the constant $a_i$ denotes the fraction of the stock related to each time scale and $\tau_i$ represents the different decay times of each sink. Table 3.1 compiles the values for the fractions and decay times of each sink, as was used in the model.

$$IRF_{CO_2}(t) = a_{CO_2,0} + \sum_{i=1}^{n} a_{CO_2,i} \cdot e^{\frac{-t}{\tau_{CO_2,i}}},\ t \geq 0. \tag{3.2}$$

**Table 3.1:** Impulse response function coefficients for the different timescales of the system, adapted from Joos et al. (2013).

| $i$ | 1 | 2 | 3 | 4 |
|---|---|---|---|---|
| $a_i$ | 0.2173 | 0.2240 | 0.2824 | 0.2763 |
| $\tau_i$ [yr] | - | 394.4 | 36.54 | 4.304 |

To compute the response of an input signal applied to a system in the time domain, the convolution operator is applied. By the convolution, previous inputs are taken into regard as $CO_2$ stock added in the past still may remain in the atmosphere and has yet to decay, which ultimately affects the total output after a given time. The added stock of $CO_2$ is as such computed through the convolution of the IRF and the unit impulse emission, according to the convolution integral described in Equation 3.3. The integral produces a point-wise product between the time series of emissions and the system IRF by shifting and scaling the input signal $f(t)$ according to the IRF $g(t)$. Equation 3.4 portrays how the convolution integral is used to obtain the added stock of $CO_2$ from an emission, as described by Gasser et al. (2017).

$$(f * g)(t) = \int_{-\infty}^{\infty} f(\tau)g(t-\tau)\ d\tau \tag{3.3}$$

$$CO_2(t) = \int_{t_0}^{t} e(t') \cdot IRF_{CO_2}(t-t')dt' + CO_2(t_0) \tag{3.4}$$

As the input to the system is an impulse, the output will simply follow the dynamics of the system given by the IRF. In practice the convolution integral could as such be computed in the model by splitting it into multiple differential equations for each of the addends in the summation given by the IRF. A mathematical connection between the expression of a convolution integral (applied to the carbon cycle) as a differential equation is shown by Enting (2007). In the model the $CO_2$ stock could as such be calculated according to Equation 3.5.

$$x_j(t) = (e_{CO_2}(t) \cdot \alpha_i + x_{j-1}e^{(-\frac{t}{\tau_i})}) \tag{3.5}$$

Having calculated the increase of atmospheric $CO_2$ stock, the resulting increase of the atmospheric $CO_2$ concentration $\Delta\rho_{CO_2}$ was calculated. By utilising the molecular mass $M_{CO_2}$ of $CO_2$, the average molecular mass of the atmosphere $M_{atm}$ as well as the mass of the atmosphere $m_{atm}$, the added concentration could simply be calculated according to Equation 3.6.

$$\Delta\rho_{CO_2} = \Delta CO_2 \frac{M_{atm}}{m_{atm} \cdot M_{CO_2}} \tag{3.6}$$

For the final step the induced effective radiative forcing associated with the increase of the atmospheric $CO_2$ concentration was calculated. This was done by applying the radiative efficiency of $CO_2$ in terms of its concentration in parts per billion

(ppb). The efficiency was derived from Forster et al. (2021) and is quantified as $re_{CO2} = 1.33 \cdot 10^{-5}$ $\mathrm{Wm^{-2}ppb^{-1}}$.

### 3.1.2 Two-box layer temperature model

To estimate the change in global temperature based on a net ERF increase, a two-layer energy balance model for climate emulation was used, based on the emulator used by (Smith et al. 2021). Figure 3.2 shows the logic of the energy balance model, which partly is defined by the temperature exchange between the mixed ocean layer and the deep ocean layer. A change in atmospheric forcing $\Delta F(t)$ affects the temperature of the mixed ocean layer, which has an average global depth of the in the range of 50-100m. Rapid heat uptake in the mixed layer is driven by convection and turbulence caused by the wind, whereas it's new temperature is further dependent on the temperature exchange between both ocean layers and heat loss to space (Johansson 2020). Just as for the carbon cycle model, the energy balance model is calibrated based on the response of comprehensive models. The parameters which define the applied model in this study is equal to those presented by Smith et al. (2021). It is assumed that the mixed ocean layer temperature is equal to the global surface air temperature.

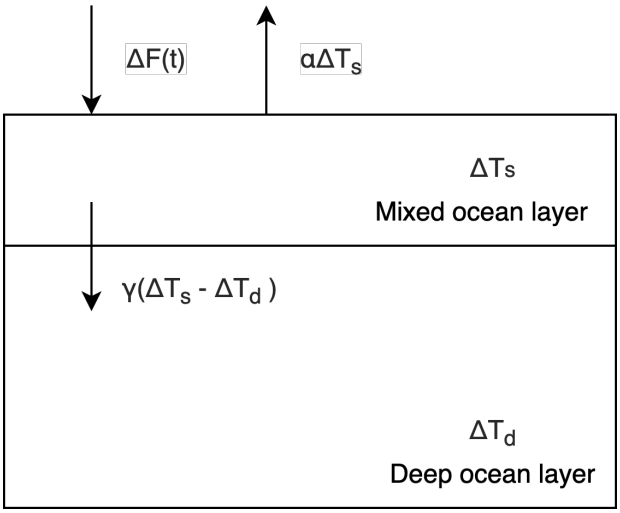


**Figure 3.2:** The figure shows the concept of the two-box layer temperature model. A change in forcing $\Delta F(t)$ is asserted on the mixed (surface) layer of the ocean, which in turn affects the temperature of the mixed layer. The final temperature of the mixed layer is further dependent on the heat lost to space as well as the heat exchanged to the deep ocean.

The change in surface temperature was modeled based on two differential equations, according to the above figure. Equation 3.7 describes the temperature change of the mixed layer $\Delta T_s$ and Equation 3.8 of the deep layer $\Delta T_d$. The heat exchange between both layers is described by the heat uptake efficacy $\epsilon$ of the deep layer and the heat transfer coefficient $\gamma$ between both layers. The effective heat capacities, which describes the heat needed to produce a change in temperature, of both ocean

layers are given by $C_t$ and $C_d$. The heat loss to the atmosphere is described by the relative damping $\alpha$. The value of each parameter as used in the model is presented in Table 3.2.

$$C\frac{d}{dt}\Delta T_s = \Delta F(t) + \alpha\Delta T_s - \epsilon\gamma(\Delta T_s - \Delta T_d) \tag{3.7}$$

$$C_d\frac{d}{dt}\Delta T_d = \gamma(\Delta T_s - \Delta T_d) \tag{3.8}$$

**Table 3.2:** Values of parameters used to model the global surface temperature change (Smith et al. 2021).

| Parameter | Value | Unit |
|---|---|---|
| $\alpha$ | -1.31 | $[Wm^{-2}K^{-1}]$ |
| $\epsilon$ | 1.03 | - |
| $\gamma$ | 0.85 | $[Wm^{-2}K^{-1}]$ |
| $C_t$ | 7.7 | $[W \cdot yr \cdot m^{-2}K^{-1}]$ |
| $C_d$ | 147 | $[W \cdot yr \cdot m^{-2}K^{-1}]$ |

### 3.1.3 Estimating ERF from contrails

The total radiative effect of contrail cirrus was estimated based on the annual $CO_2$ emissions related to Swedish bunkering of jet fuel. A ratio of the radiative efficacy of contrails in relation to $CO_2$, was derived from Lee et al. (2021). The used radiative efficacy was given as 0.0555 $\mathrm{mWm^{-2}\ Tg_{CO_2}{}^{-1}}$.

### 3.1.4 Reduction of ERF due to SAF

For iterations in the model for in which the reference Jet A1 fuel is complemented by any percentage of drop-in fuel, both the ERF from $CO_2$ and contrail cirrus had to be adjusted. The emission index of blended fuel was dynamically changed based on the relationship presented by Klöwer et al. (2021), seen in Equation 3.9. Where $m$ denotes the share of Jet A1 fuel and the share of biofuel in the blended fuel is given by $1 - m$. The updated amount of $CO_2$ could then be applied to the carbon cycle model to attain the relevant forcing.

$$\text{Emission index} = 3.16m\ \mathrm{kgCO_2\ kg^{-1}fuel} \tag{3.9}$$

In the case of contrail ERF, a relationship was established for the percentage of SAF and the change in ERF due to a reduction of the fuel aromatic content, based on results presented in the studies by Burkhardt et al. (2018) and Voigt et al. (2021). The relationship was composed of 5 succeeding steps, seen in Figure 3.3, spanning from the share of biofuel to the following reduction of aromatic content, soot particles, ice crystal numbers and lastly the resulting updated ERF.

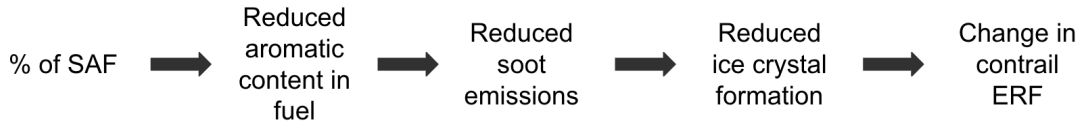


**Figure 3.3:** The logic behind how the application of SAF changes the ERF of contrails.

To determine a relationship between the share of SAF mixed in with in kerosene-based jet fuel and how it modifies the overall fuel composition, it was necessary to gather specific data about the fuel properties of SAF. The ECLIF1 and ECLIF2/ND-MAX experiments on fuel burn of different jet fuels were used as a reference, as they included the properties of jet fuel blends containing SAF as well as details about particle emissions during combustion of these fuels. In particular two fuel blends from the tests (ref2 and SAF1) were adapted in this study, seen in Table 3.3. The 100% Jet A1 fuel is a typical kerosene jet fuel blend without treatment to reduce aromatics or naphthalenes. The investigated sustainable fuel is a blend of 51% Jet A1 fuel and 49% bio-based HEFA-SPK. It was assumed that the Jet A1 fuel properties of both fuel blends were identical, although there existed a slight discrepancy in the aromatic content between the two (Voigt et al. 2021).

**Table 3.3:** Composition of the reference Jet A1 fuel and blended fuel used in the study. Fuel properties are sourced from Voigt et al. (2021).

| Composition | 100% Jet A1 | 51% Jet A1 & 49% HEFA-SPK | Unit |
|---|---|---|---|
| Aromatics | 17.2 | 8.5 | vol% |
| Naphthalenes | 1.83 | 0.61 | vol% |
| Hydrogen content | 13.73 | 14.4 | mass% |
| H:C ratio | 1.9 | 2 | mass% |
| Specific energy | 43.2 | 43.63 | MJ/kg |
| Sulfur total | 0.135 | 0.007 | mass% |
| Particle number emissions | $4.2{\cdot}10^{15}$ | $2.7{\cdot}10^{15}$ | kg fuel$^{-1}$ |

Based on the properties of the two reference fuels presented above, a number of linear relationships could be established between the properties of both fuel blends and the share of SAF. Firstly, a linear relationship between the aromatic content and percentage of HEFA-SPK was derived, resulting in a reduced aromatic content of 0.1775% per percent of dropped-in HEFA-SPK. Similarly, it was derived that reducing the aromatic content by one percent would reduce soot emissions by a number of approximately $2.53{\cdot}10^{14}$ particles. The reduction of soot particles is estimated to yield an equal reduction in ice crystal numbers, however after the contrail vortex phase a 10% loss of ice crystal numbers was assumed (Burkhardt et al. 2018). The reduction of ice crystals $R_{ice}$ is described by Equation 3.10 where $m$ denotes the share of SAF between 0-100%. $R_{aromatics}$ and $R_{soot}$ denotes the respective reduction of aromatics and soot. By using a reference number of ice

crystals pertaining to 100% Jet A1, as measured in the ECLIF1 and ECLIF2/ND-MAX experiments, the new ice crystal numbers for the blended fuel containing any percentage of HEFA-SPK was then obtained by the subtracting the calculated reduced ice crystal numbers $R_{ice}$ from the reference number. Reference ice crystal numbers were estimated as $4.2{\cdot}10^{15}$ per kg fuel.

$$R_{aromatics} \cdot R_{soot} \cdot 0.9 \cdot m = R_{ice} \tag{3.10}$$

A relationship between the fraction of reduced ice particle numbers and the subsequent reduction in ERF of contrails was adapted from Burkhardt et al. (2018). From this relationship it follows that the fraction of reduced ice crystal numbers in relation to the reference fuel ice crystal numbers, approximately reduces the ERF by the square of the reduced fraction. The data points in Figure 3.4 displays this relationship as adapted from Burkhardt et al. (2018).

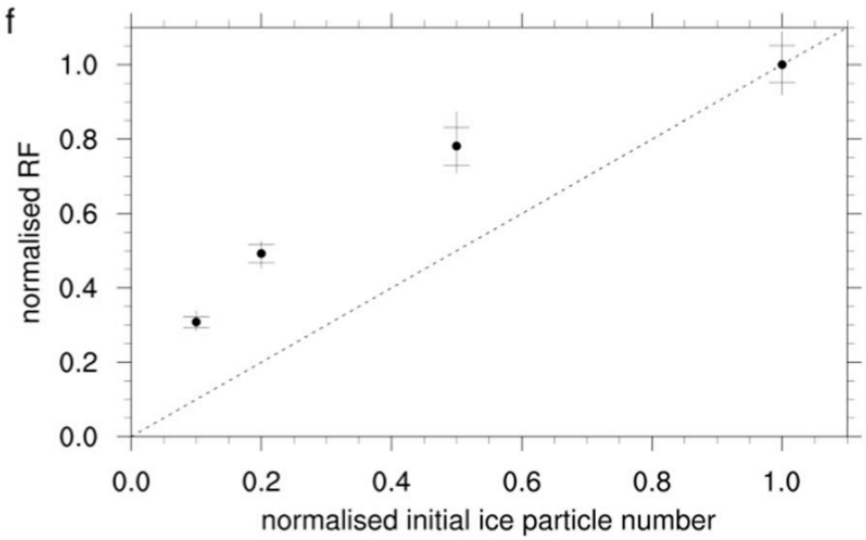


**Figure 3.4:** The reduction of ice particle numbers in relation to current emissions and the induced change in radiative forcing *Source:* Burkhardt et al. (2018) (CC BY 4.0).

The above dependencies were compiled into one expression. The resulting ERF caused by contrails, for a given share of SAF $m$ blended with Jet A1, is depicted in Equation 3.11. Current (reference) ice crystal numbers were assumed to be as that of the reference Jet A1 fuel as quantified previously.

$$ERF = \sqrt{\frac{ref_{ice} - 4.041 \cdot 10^{13} m}{ref_{ice}}} \cdot ERF_{fossil} \tag{3.11}$$

### 3.1.5 Accounting for carbon cycle feedback

The temperature response given by the contrail induced forcing affects the carbon sinks through outgassing of carbon to the atmosphere, with an intensity that decreases with time (Gasser et al. 2017). The response of the carbon sinks to an increase of temperature was modeled by an impulse response function. Equation 3.12 describes the dynamics of the carbon net flux $\Delta F$. The temperature change is modeled as an impulse which is applied to the response function of the carbon sinks. The response to the impulse is given by the IRF of the carbon cycle feedback and the intensity parameter $\gamma$, which describes the $CO_2$ temperature response and is given as $1.1{\cdot}10^{10}$ $tCO_2$ $K^{-1}$ $year^{-1}$.

$$\Delta F(t) = \gamma \int_{t_0}^{t} [T(t') - T(0)] \cdot IRF_{cc}(t - t')dt' \tag{3.12}$$

The IRF of the carbon cycle feedback was derived from Gasser et al. (2017) which was estimated using the Earth system model OSCAR. The response function is largely similar to the one used to calculate the response for $CO_2$ emissions and is similarly made up of decaying exponential functions. The annual response to an impulse, as determined by Gasser et al. (2017), is given by Equation 3.13. The IRF can as such be summarised according to Equation 3.14.

$$x'(t) = \gamma(\alpha_1 \exp(-\frac{t}{\tau_1}) + \alpha_2 \exp(-\frac{t}{\tau_2}) + \alpha_3 \exp(-\frac{t}{\tau_3})) \tag{3.13}$$

$$IRF_{cc}(t) = \sum_{i=1}^{n} a_i \cdot e^{\frac{-t}{\tau_i}},\ t \geq 0 \tag{3.14}$$

The applied parameters for the IRF as used in the model are given in Table 3.4, where $a_i$ denotes the fraction of outgoing carbon flux for each sink and $\tau_i$ again expresses the timescale.

**Table 3.4:** Impulse response function coefficients for the different timescales of the system, adapted from (Gasser et al. 2017; Smith et al. 2021).

| $i$ | 1 | 2 | 3 |
|---|---|---|---|
| $a_i$ | 0.6368 | 0.3322 | 0.031 |
| $\tau_i$ [yr] | 2.376 | 30.14 | 490.1 |

## 3.2 Python implementation of climate model

The Python implementation of the climate model was separated into multiple modules and followed the structure shown in Figure 3.1. The interaction between modules was designed to be a flow of list data types. Each item in the lists represented a certain parameter pertaining to a specific year which was given by the indexation of the list. A list of data would be fed into a module, where the data would be used to

perform the necessary computations according to the described methodology. A new list containing the computed data would then be returned to be used by another module for the next step of the calculations. Parameters such as timescales and efficacies were implemented as global variables, making the model easy to modify in case of need to update any parameter.

### 3.2.1 Initialisation

Running the model started with initialisation of the scenarios which were to be modeled. Each scenario was built separately but through the same procedure, as described further in Chapter 4. Annual emissions for each scenario were derived from local text files which were created for each scenario, based on the separate scenario construction. The text files could then be read and saved into scenario-specific lists during the initialisation stage. These lists in turn defined the $CO_2$ pulse emissions starting at index 0 for the scenario starting year 1973, with an incremental increase spanning to the final year 2050. The same thing was done for the share of SAF in the jet fuel for each year, which also was different from case to case depending on the scenario.

### 3.2.2 Logic of computation

The calculations performed in the model follow the same equations and relationships as presented previously. The impulse responses of the carbon cycle and carbon cycle feedback to $CO_2$ pulses were calculated to account for the cumulative emissions in respect to each sink. In practice each sink was treated as a separate box and the change in stock was calculated for each box individually for the given year. The new atmospheric stock of $CO_2$ was then obtained by summation of all boxes as portrayed in Figure 3.5 and the result pertaining to each year during the time span was stored in a list.

$$x'(t) = \underbrace{(e \cdot \alpha_0 + c0)}_{\text{Box 1}} + \underbrace{(e \cdot \alpha_1 + x_1 e^{(-\frac{t}{\tau_1})})}_{\text{Box 2}} + \underbrace{(e \cdot \alpha_2 + x_2 e^{(-\frac{t}{\tau_2})})}_{\text{Box 3}} + \underbrace{(e \cdot \alpha_3 + x_3 e^{(-\frac{t}{\tau_3})})}_{\text{Box 4}}$$

**Figure 3.5:** Obtaining the new atmospheric $CO_2$ stock (tonnes) after a perturbation $e$, by adding the response of each sink.

The concentration of atmospheric $CO_2$, quantified in parts per billion, was then derived for each year based on the $CO_2$ stock of each year as described previously. The list of annual concentrations could then be iterated through and multiplied with the radiative efficiency of $CO_2$ in order to obtain the change in ERF for each year. Contrails ERF could simply be calculated directly from the $CO_2$ emission data read from the text files. The contrails ERF could then be adjusted accordingly based on the relationship derived in Equation 3.11 and in accordance with the specific share

of SAF enforced by the reduction obligation quota from 2021 and forwards.

The energy balance model worked in a structurally similar way and was implemented according to the two differential equations presented earlier in Section 3.1.4. By providing a list of forcings to the module, the change in global mean surface temperature $\Delta T_s$ was determined for each year by computing the differential equations with the given forcings, which were derived in the previous step.

### 3.2.3 Utilised libraries

Performing mathematical computations in Python could be done by utilising the NumPy library which contains a vast variety of mathematical functions. In addition, the library matplotlib was applied in the final step of the model when it came to visualizing all of the output data which was stored within the lists pertaining to each scenario.

# 4 | Scenarios

Different scenarios for the future of Swedish aviation have been looked at to get an understanding about the potential climate impact associated with different future outcomes related to the aviation industry. In total, 12 scenarios have been investigated. These are centered around 3 different outlines of aviation growth and are named as the Reference-, Zero growth- and Transition scenarios, which are described further in Section 4.2. For the scenarios this growth was related to the growth rate of fuel bunkering at airports in Sweden. In addition, the variability of technological advancements, in terms of energy efficiency within the industry, are accounted for in the scenarios. Furthermore, the future of sustainable aviation fuels as a jet fuel alternative to fossil-based jet fuel is considered. Emissions related to each scenario are based on in-flight circumstances of fuel combustion and does as such not account for emissions from a life cycle perspective, e.g. from resource extraction, fuel manufacturing as well as transportation.

## 4.1 Trends in the development of aviation

### 4.1.1 Recovery of pre-pandemic flight volumes

The COVID-19 pandemic came with a drastic reduction in both global and Swedish flight volumes at the beginning of 2020. ICAO describes the overall global capacity of seats offered by airlines to have been halved in 2020 and still be down by 40% during 2021 (Toru 2021). In Sweden, the number of departing passengers at the airports decreased by 75% in 2020, in relation to the previous year (Transportstyrelsen 2021). The time it will take for flight volumes to be restored to pre-pandemic levels is uncertain. A forecast done by Transportstyrelsen (2021) even outlines an overall reduction of air travel in respects to previous levels after recovery, although this estimation leaves room for questioning (Larsson et al. 2021). The International Air Transport Association (IATA) instead predicts international flight volumes to be restored by 2025, whereas they expect aviation within Europe to return to previous levels as soon as in 2024 (IATA 2022). Both Eurocontrol and Swedavia expect a recovery first after 2025 (Larsson et al. 2021).

In this study it has been assumed that flight volumes will be restored to pre-pandemic levels by 2025, which is in line with the assumptions made by Larsson et al. (2021) in their report on a consumption-based scenario analysis of Sweden.

### 4.1.2 Growth of Swedish aviation

When it comes to Swedish bunkering of jet fuel there has been an increase of 44% in total jet fuel usage in the past three decades. Fuel usage volumes have grown from a total of 940,000 cubic meters to 1,360,000 cubic meters (SOU 2019), as depicted in Figure 4.1. The fueling related to departure from Swedish airports can be further divided into domestic and international flights. The growth of bunkering related to domestic departures has stagnated during the last decade and seen an overall decrease since 1990, with an historic annual growth of −1.3% between 1990-2019, based on the data from Energimyndigheten (2020). On the other hand, fuel usage for international departures from Swedish airports has increased annually at a rate of 2.5% during the same time period.


**Figure 4.1:** Development of fuel bunkering in Sweden between 1990-2019. Data sourced from Energimyndigheten (2020).

The historic growth rate shows a drawn out decrease in domestic flight volumes, with close to a standstill but minimal increase in volumes between 2010 and 2017. However, in the most recent years, the fuel usage again exhibits as downwards sloping trend. The effect that the pandemic will have on domestic departures is unsure. A substantial part of domestic flights in Sweden, approximately 60%, are associated with business trips (Larsson et al. 2021). As a result of digital meetings having become increasingly normalised due to the pandemic it is possible that domestic flight volumes will decrease further below pre-pandemic levels due to behavioral change. This reduction could be at a level of 30% below 2019 flight volumes, according to Luftfartsverket (Larsson et al. 2021). Whether or not this is the most likely development is uncertain (Transportstyrelsen 2021), some estimates made before the pandemic assumed an annual passenger increase for domestic flights. Trafikverket estimated an annual passenger increase of 0.5% up until 2040, with low and high estimates being 0% and 1%. Similarly, Swedavia had estimates of 0.2%, 0.8% and 1.2% for domestic annual passenger increase (SOU 2019).

In the case of international flight volumes, a lower fraction of flights are associated with business related travel, Larsson et al. (2021) estimate this number to be around

20%. Per capita, international travel has increased historically at a rate of 2.9% per year (Kamb and Larsson 2019). Pre-pandemic estimates of future flight volumes by Trafikverket and Swedavia assumes a continued increase, where all projections fell somewhere in between 1% and 3.7% (SOU 2019).

For all of the scenarios which have been investigated this study, growth related to the fuel usage of domestic departures is assumed to be at a rate of $-1.3\%\ \mathrm{yr}^{-1}$ and thus in line with the historic growth rate. The domestic flight volumes are estimated to return to 2019 levels by 2025 and decrease throughout the post-pandemic years up until 2050. The growth of bunkering related to international departures will vary according to scenario-specific aspects presented in the scenario definitions.

### 4.1.3 Improvements in rate of efficiency

There is a slower increase of emissions in relation to the growth in flight volumes, meaning revenue passenger kilometers (RPK) is growing faster than the use of jet fuel (Lee et al. 2021). This can be attributed to efficiency gains within the aviation industry, which mainly is due to more effective load capacities, keeping the airplanes with as few empty seats as possible (Naturvårdsverket n.d.[a]). Moreover, technological advancements in fuel- and engine mechanics as well as larger aircrafts are also factors which improve the efficiency of aircraft. Historically, energy efficiency improvements have been at an annual rate of approximately 1.9% between the period of 1990-2017 (Kamb and Larsson 2019). Klöwer et al. (2021) states that future efficiency potential is limited, however it is difficult to estimate exact future rates. Flemming and Lépinay (2019) sees a moderate scenario of fuel efficiency to be situated at yearly improvements of 0.96% up until 2050 and an optimistic view to be of 1.5% per year. ICAO has a goal of reaching 2% fuel efficiency per year, a goal which is described as ambitious (Flemming and Lépinay 2019; Terrenoire et al. 2019).

In this study two rates of energy efficiency have been investigated. The first being $1\%\mathrm{yr}^{-1}$ and thus in line with the moderate outlook of fuel efficiency. Secondly, a rate portraying the historic growth rate and potential of a high energy efficiency rate is also investigated. An annual rate of $1.9\%\mathrm{yr}^{-1}$ was chosen as this follows the previous development.

### 4.1.4 Implementation of alternative fuel blends

The transition to more sustainable jet fuel blends began in Sweden during 2021 after the implementation of Reduktionsplikten. The reduction obligation quota requires jet fuel suppliers in Sweden to reduce greenhouse gas emissions associated with the fuel they provide by usage of sustainable drop-in fuels. The annual amount of required reductions is shown in Table 4.1, where the predicted share of necessary SAF also is presented. The increase in reductions is set to end in 2030 with a target of reaching a 27% reduction of greenhouse gas emissions, from a life cycle perspective. Contrary to SOU (2019), in this study it is assumed that production

related emissions of both bio-based and fossil jet fuel are equal in size. As such differences related to the share of drop-in fuel solely affects end-of-pipe emissions upon fuel usage. In the reduction obligation quota the share of SAF starts out slow with minor levels of build up during the initial years. This is stated to be because of uncertainties pertaining to the market of SAF and how the global supply and demand of sustainable fuels will evolve (SOU 2022). On an EU-level the RefuelEU Aviation program is proposed to implement a renewable fuel quota, although at a slower pace than the Reduktionsplikten program in Sweden. The proposed share of SAF by 2030 is set as 5% in the RefuelEU Aviation program with a final goal of reaching a share of 63% in 2050 (SOU 2022).

**Table 4.1:** Levels of mandatory reduction in greenhouse gas emissions per year and the estimated share of SAF necessary to reach the required reduction level (SOU 2019).

| | 2021 | 2022 | 2023 | 2024 | 2025 | 2026 | 2027 | 2028 | 2029 | 2030 |
|---|---|---|---|---|---|---|---|---|---|---|
| Reduction [%] | 0.8 | 1.7 | 2.6 | 3.5 | 4.5 | 7.2 | 10.8 | 15.3 | 20.7 | 27 |
| SAF vol. [%] | 1 | 2 | 3 | 4 | 5 | 8 | 12 | 17 | 23 | 30 |

A Swedish roadmap exists for making aviation fossil-free by 2045 and already by 2030 for domestic flights (SOU 2022). While not a part of the reduction obligation quota, the climate effect of 100% fossil-free jet fuel by 2045 has been investigated in this study to understand its potential from a climate impact perspective, as well as the current stipulation of a 27% reduction by implementing a share of 30% SAF. As such this is applied for all scenario variations.

## 4.2 Scenario definitions

### 4.2.1 Reference scenario

The reference scenario is formalized to portray the future development of the Swedish aviation industry when in line with historic growth rates. As such the growth of fuel bunkering related to international departures continues at a pace of 2.5% per year after 2025 when pre-COVID-19 levels of travel is assumed to be have been restored. The growth of domestic travel is predicted to continually decline at an annual rate of $-1.3\%$, as for all of the investigated scenarios. Technological and logistical advancements leading to improvements in energy efficiency is also set up to follow past levels of growth. This efficiency is estimated to follow an annual improvement of $1.9\%\text{yr}^{-1}$. In the reference scenario there are also no further climate incentives introduced which would aim to alter the climate impact of the Swedish aviation industry, otherwise than those already in place. The reduction obligation quota is implemented according to current stipulations and stops in 2030 with a total share of 30% drop-in fuel. In alterations of the reference scenario the second rate of efficiency and the 100% SAF perspectives are however also investigated.

### 4.2.2 Zero growth scenario

The zero growth scenario depicts a future in which there is no further growth of international departures at Swedish airports. After recovery of pre-pandemic flight volumes this means that fuel bunkering will remain at a constant level, whereas overall emissions still are affected by the increasing share of drop-in fuels and efficiency improvements. The effect of the pandemic in itself could work as an influential factor on behavioral change and for arriving at the described outcome. Digital meetings in the workplace could prove to reduce international business trips and domestic holidays could become more prominent as stricter rules for international travel might have incentivised people to explore local areas during the pandemic. Increased climate awareness could further stimulate behavioral change in the travel habits of the population. A future in which stricter policies are targeted towards the aviation industry could also be a potential outcome as to reduce future aviation volumes e.g. by form of increased carbon taxation.

### 4.2.3 Transition scenario

The transition scenario exemplifies a future for which aviation as a means of travel decreases or is drastically modified. After flight volumes are restored for the post-pandemic development, a linear decrease totalling 30% of international departures is assumed to transpire between the years of 2025 and 2050. As such, linearly reducing the associated emissions of bunkering volumes by 30%, not including reductions stemming from efficiency gains and use of SAF during the same time period.

Research by Åkerman et al. (2021) investigates different scenarios which would constitute a large decrease in emissions from long-distance travel in line with limiting global warming to an increase of 1.8°C, focusing on air travel. As travel by air is the predominant method of travel over great distances, one of the explored options includes a modal shift towards high speed railways, something which would be technically feasible within Europe. Time spent travelling in comparison to flying is a potential constraint and a change in consumer behaviour where longer travel times are more customary. Åkerman et al. (2021) remarks that targeting the shorter trips done by air through policy regulation could be one such avenue as to induce a change in travel habits.

Other pathways presented by Åkerman et al. (2021) to drastically reduce emissions are directed more heavily towards the aviation industry. Technological changes such as transitioning engine technology towards open rotor specifications rather than the currently used turbofan engines could lead to reduced fuel usage by up to 20%. Rerouting flight trajectories could also limit the formation of persistent contrails and as such the climate impact associated with their effect on the radiative balance of the Earth. It is noteworthy that open rotor configurations reduces the velocity of aircraft and would as such increase travel time. The same predicament is true of rerouting air traffic, by effect of leading to longer travel itineraries. Providing appropriate incentives or regulations for the airlines would therefore need to be considered.

Construction of high speed railways and implementation of new aircraft technologies are both two demanding procedures in terms of time before completion and thus being able to utilise the change. Work towards realising the shift would have to start swiftly and could be seen as optimistic to realise within the investigated time frame. Transitions of this type and scale would also require considerable international collaboration in order to realise. It is possible that a future which facilitates the stated reduction in emissions is constituted by a combination of said pathways, where each option to transform long-distance travel is implemented to a lesser extent than if it were to be the sole focal point of a transition. On top of the significant change in flight volumes, this scenario also includes the current stipulations of implementation of sustainable aviation fuels as an addition to the transition of travel related to international departures.

### 4.2.4 List of scenarios

In line with the described scenario definitions above and the possible variations of deciding factors which would alter the given climate impact of aviation, 12 different scenarios have been produced to represent the variability of future parameters and how their change can impact the future climate. The scenarios are presented in Table 4.2. The letters H and L denotes a high and low rate of energy efficiency improvements, whereas the numbers 30 and 100 denotes the total SAF content arrived at in 2050.

**Table 4.2:** The 12 scenarios which are investigated in the study, centered around the base cases Ref, ZeroGrowth and Transition, which describe the projected flight volume growth rates.

| Scenario | Aviation growth [$yr^{-1}$] | Energy efficiency [$yr^{-1}$] | SAF content [vol%] |
|---|---|---|---|
| Ref (1) | 2.5% | 1.9% | 30% |
| $Ref^{H}_{100}$ (2) | 2.5% | 1.9% | 100% |
| $Ref^{L}_{30}$ (3) | 2.5% | 1% | 30% |
| $Ref^{L}_{100}$ (4) | 2.5% | 1% | 100% |
| $ZeroGrowth^{H}_{30}$ (5) | 0% | 1.9% | 30% |
| $ZeroGrowth^{H}_{100}$ (6) | 0% | 1.9% | 100% |
| $ZeroGrowth^{L}_{30}$ (7) | 0% | 1% | 30% |
| $ZeroGrowth^{L}_{100}$ (8) | 0% | 1% | 100% |
| $Transition^{H}_{30}$ (9) | -1.5% | 1.9% | 30% |
| $Transition^{H}_{100}$ (10) | -1.5% | 1.9% | 100% |
| $Transition^{L}_{30}$ (11) | -1.5% | 1% | 30% |
| $Transition^{H}_{100}$ (12) | -1.5% | 1% | 100% |

## 4.3 Scenario construction

The scenarios were built using the spreadsheet software Excel. The total amount of fuel used, related to departures from Swedish airports, was required in order to calculate the total $CO_2$ emissions for each year. Historic energy use for aviation within the Swedish transport sector was gathered from Energimyndigheten and included both domestic- and international travel data. The collected data was in terms of the volume ($1000m^3$) of used jet fuel and represented fuel use pertaining to fuel bunkering. All fuel was assumed to be of a homogeneous Jet A1 type. $CO_2$ emissions associated with the fuel use could be obtained through utilising the density and emission index of Jet A1 fuel, as presented in Table 4.3.

**Table 4.3:** Parameters used to calculate the $CO_2$ emissions of bunkered fuel in Sweden. Values are derived from Lee et al. (2021) and Government of Canada (2016).

| Parameter | Value | Unit |
|---|---|---|
| Jet A1 density | 804 | [kg $m^{-3}$] |
| Jet A1 emission index | 3.16 | [kg$CO_2$ kg fuel$^{-1}$] |

Future fuel bunkering volumes were calculated according to the parameters of each specific scenario (Seen in Table 4.2). The historic data was extrapolated for the period of 2021-2050 based on the parameters for aviation growth, energy efficiency and percentage of SAF content. During the COVID-19 recovery period between 2020 and 2025, bunkering volumes were restored to 2019 levels by linear growth. The future development was then dependent on scenario related specifications.

### 4.3.1 SAF blending ratios

The share of drop-in fuel content pertaining to each year was derived from official documents regarding the reduction obligation quota. Historically, the fraction was set as zero from 1973 up until 2021. For the scenarios with a final fuel composition consisting of 30% SAF, yearly increases in SAF blending ratios were adapted according to the accepted proposition (Sveriges Riksdag 2021) and stopped at 30% in 2030. In the case of a final fuel composition consisting of 100% SAF, fuel blending was set to increase linearly from 30% in 2030 to 100% in 2045.

# 5 | Results

In the results chapter the different outcomes obtained by running the 12 scenarios in the climate model are presented. A general outlook on the climate impact is given for all of the scenarios before the focus then is shifted towards outliers amongst the scenarios, in order to investigate any particular deviation pertaining to certain parameters. The total contributing climate effect of each forcer is investigated at the conclusion of each scenario in 2050, as to paint a picture of the outcome related to the outliers. Additionally, the relationship which was established in this study in regards to the aromatic content of jet fuel and the subsequent reduced fraction of contrail ERF, is compared and evaluated against the relationships presented in the studies by Klöwer et al. (2021) and Grewe et al. (2021).

## 5.1 Attributed ERF of scenarios

Figure 5.1 displays the associated effective radiative forcing for each of the scenarios. From the figure it can be seen that the reference scenario $\text{Ref}_{30}^{L}$ gives rise to the highest increase in energy flux by the end of 2050. In turn, all of the scenarios belonging to the reference case produce a relatively high ERF in comparison to the respective counterparts of the zero growth and transition scenarios. This is to be expected due to the reference scenarios having the highest annual growth in fuel bunkering volumes out of the three base cases. The influence of a jet fuel blend exceeding 30% is also evident as scenarios with the *'100'* notation lies amongst the scenarios with the lowest attributed ERF for each of the base cases. The reduced ERF as an effect of SAF is due to the combination of reduced contrail formation but also decreased $CO_2$ emissions. The large and short term radiative effect of contrails makes it so that an increased share of SAF reduces the total ERF at a quick pace by the immediate reduction in contrail formation. The rate at which the ERF reduces levels out after the share of SAF reaches 100%. Because of the accumulation of $CO_2$ in the atmosphere, the lessened radiative effect related to reduced $CO_2$ emissions becomes more evident first over a longer period of time. It is also visible that due to the established non-linear relationship between the reduced number of formed ice crystals and the fraction of reduced ERF, higher shares of SAF becomes increasingly more influential when it comes to reducing the ERF associated with contrails. This can be seen in the figure for the scenarios pertaining to a final share of 100% SAF, as the downwards slope of the curve trajectories becomes steeper when approaching 2045.

The zero growth scenarios for the cases with a final share of 30% SAF, display the outcomes coming the closest to a static level of energy flux. This gives an idea to where the breaking point lies in terms of necessary action for reducing growth of the ERF induced by aviation fueled in Sweden, where the higher rate of efficiency shifts the ERF on a downwards trend but the lower rate sees a small increase after 2030. Appropriately, on the lower end of the spectrum lies the transition scenarios for which the reduction in ERF is the largest, being very similar for both the Transition$^{L}_{100}$ and Transition$^{H}_{100}$ scenarios.

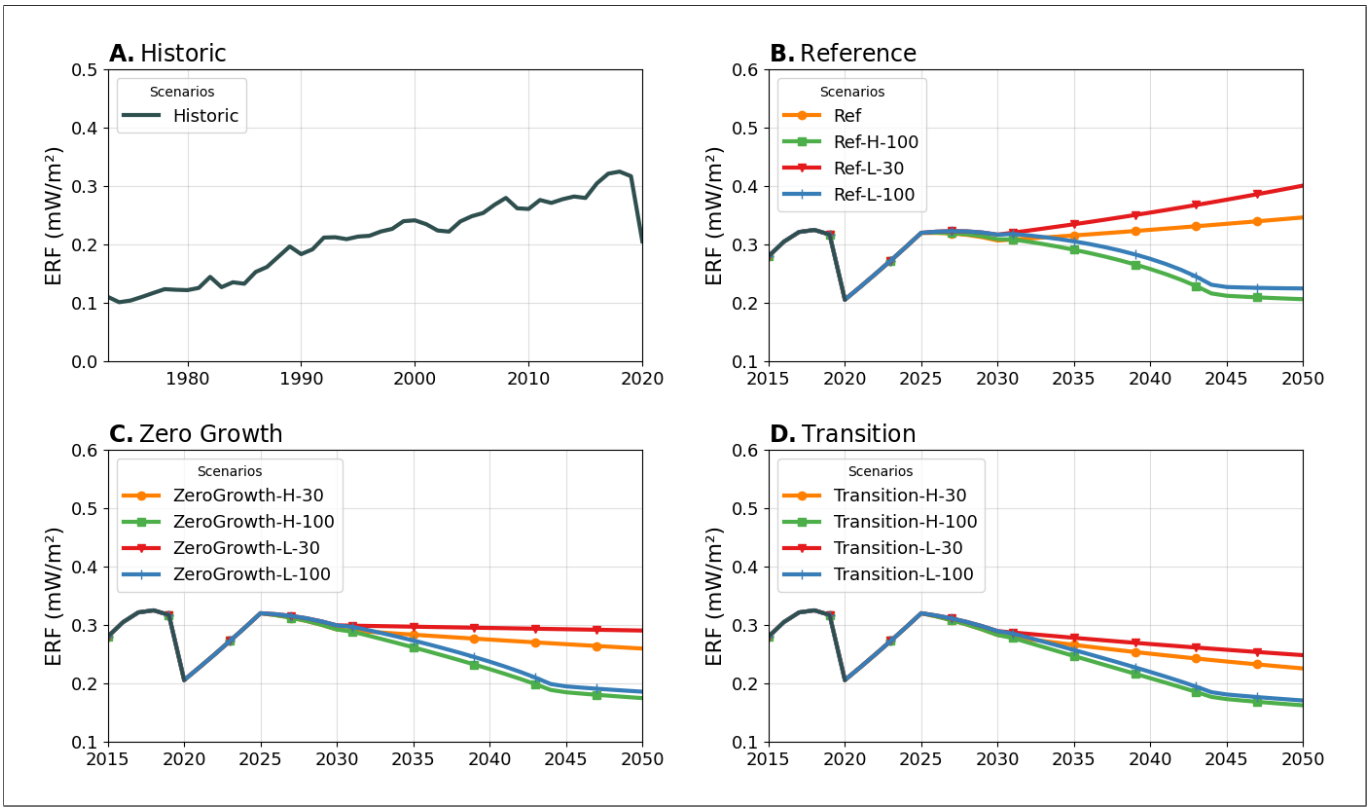


**Figure 5.1:** Compartment A displays the historic ERF from 1973 up until the pandemic in 2020 and is the precursor to the different outcomes of all scenarios. B, C and D displays the ERF for each of the 4 scenarios pertaining to each base scenario; reference, zero growth and transition and is investigated up until 2050.

The dip in quantified ERF, seen in 2020, is as a result of reduced flight volumes because of the COVID-19 pandemic. At the point of recovery to pre-pandemic flight volumes in 2025, the share of SAF in the overall jet fuel has reached a level of 5%. The short lived radiative effect of contrails and the non-linearity of historic emissions explains the roughness of the historic emissions up until 2021, which can be seen in compartment A.

## 5.2 Contribution to global warming

Figure 5.2 exhibits the temperature change which is induced by the net increase in ERF. Historic warming before the events of the pandemic reached a net increase of 0.15 mK. The continuation of the temperature change is further seen in the lower part of figure, relating to the outcome of the different scenarios. Overlap is found amongst the scenarios in terms of the resulting temperature increase but the highest warming is found in the reference scenario and the lowest in the transition scenario, which approximately is half of what the highest reference scenario gives rise to.

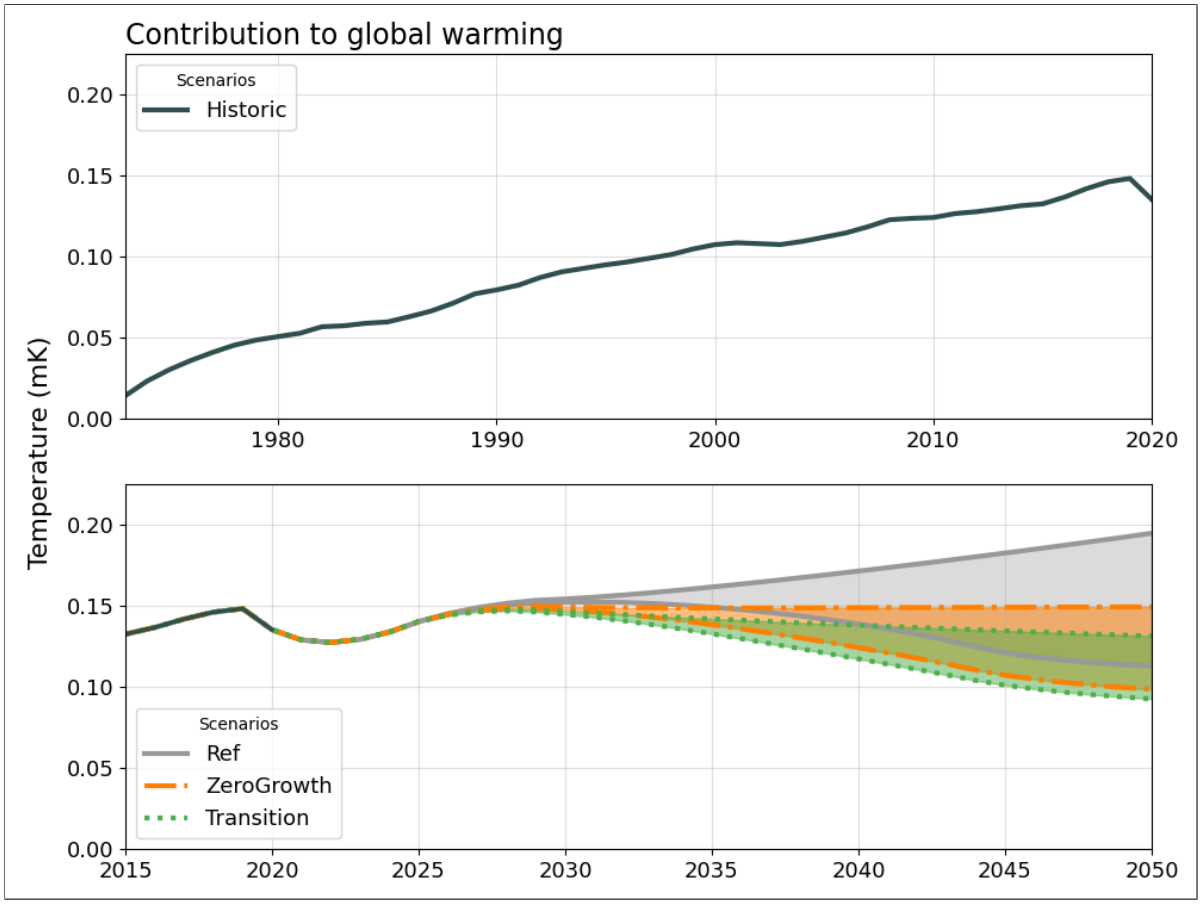


**Figure 5.2:** The upper plot shows the historic development of temperature change related to Swedish fuel bunkering between 1973 and 2020. The lower plot presents the range within which future temperatures will fall for the scenarios up until 2050.

The climate warming is further presented for 5 differing scenarios, seen in Figure 5.3. Out of the 12 scenarios, $\text{Ref}_{30}^{L}$ produces the largest warming effect at a temperature change of 0.195 mK. On the opposite side is the $\text{Transition}_{100}^{H}$ scenario with the lowest warming, having a resulting temperature change of 0.093 mK. This is approximately a 53% decrease in relation to $\text{Ref}_{30}^{L}$.

Between the edge cases, 3 other scenarios are also seen; $\text{Ref}_{100}^{L}$, $\text{ZeroGrowth}_{30}^{L}$ and $\text{Transition}_{30}^{H}$. Although the reference-based scenario $\text{Ref}_{100}^{L}$ starts off as the most

significant in terms of warming, by 2040 it falls below the ZeroGrowth$^{L}_{30}$ scenario and by 2045 it is on par with Transition$^{H}_{30}$ in terms of warming. The results indicate how even for the higher rate of passenger growth and lower rate of efficiency gains, the potential of 100% drop-in fuel is considerable as it equals the warming effect of the high efficiency and lower passenger volumes of Transition$^{H}_{30}$. In addition, Table 5.1 summarizes the temperature response associated with each of the scenarios for the final year 2050.

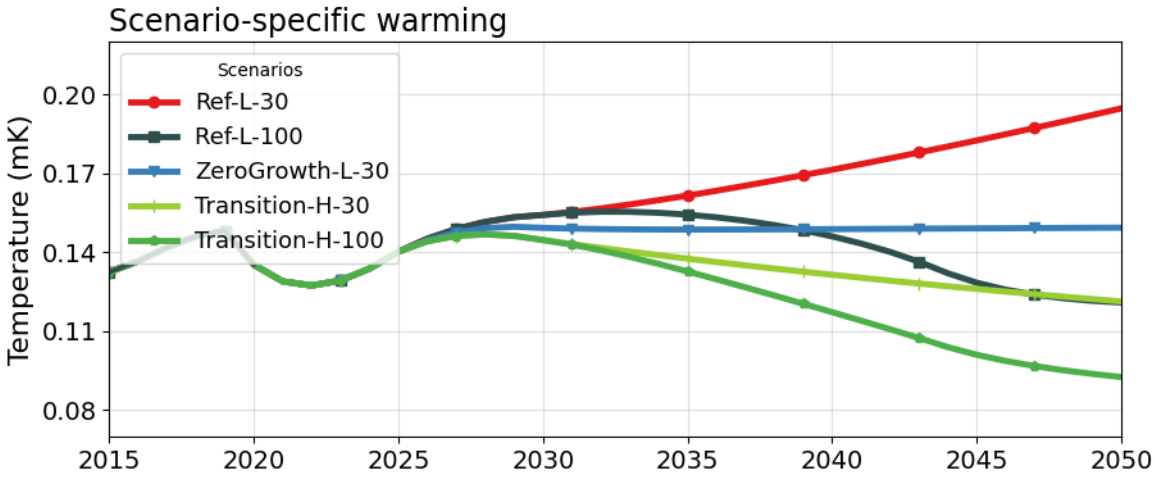


**Figure 5.3:** The temperature response of the edge case scenarios Ref$^{L}_{30}$ and Transition$^{H}_{100}$, as well as 3 scenarios portraying the variability in between depending on the applied parameters.

**Table 5.1:** Compilation of the resulting temperature response at 2050 for all of the investigated scenarios.

| Scenario | Temperature response [mK] |
|---|---|
| Ref (1) | 0.172 |
| Ref$^{H}_{100}$ (2) | 0.113 |
| Ref$^{L}_{30}$ (3) | 0.195 |
| Ref$^{L}_{100}$ (4) | 0.120 |
| ZeroGrowth$^{H}_{30}$ (5) | 0.136 |
| ZeroGrowth$^{H}_{100}$ (6) | 0.098 |
| ZeroGrowth$^{L}_{30}$ (7) | 0.149 |
| ZeroGrowth$^{L}_{100}$ (8) | 0.104 |
| Transition$^{H}_{30}$ (9) | 0.121 |
| Transition$^{H}_{100}$ (10) | 0.093 |
| Transition$^{L}_{30}$ (11) | 0.131 |
| Transition$^{H}_{100}$ (12) | 0.096 |

## 5.3 Most prominent climate forcer

To understand the change in distribution of the emissions for the given scenarios, a closer look of the different climate forcers is presented in Figure 5.4. The two bar charts gives a breakdown of how much the investigated climate forcers contribute to both the effective radiative forcing and the warming effect of the five previously shown scenarios, as well as the respective fractions for 2019 before the different scenarios play out.

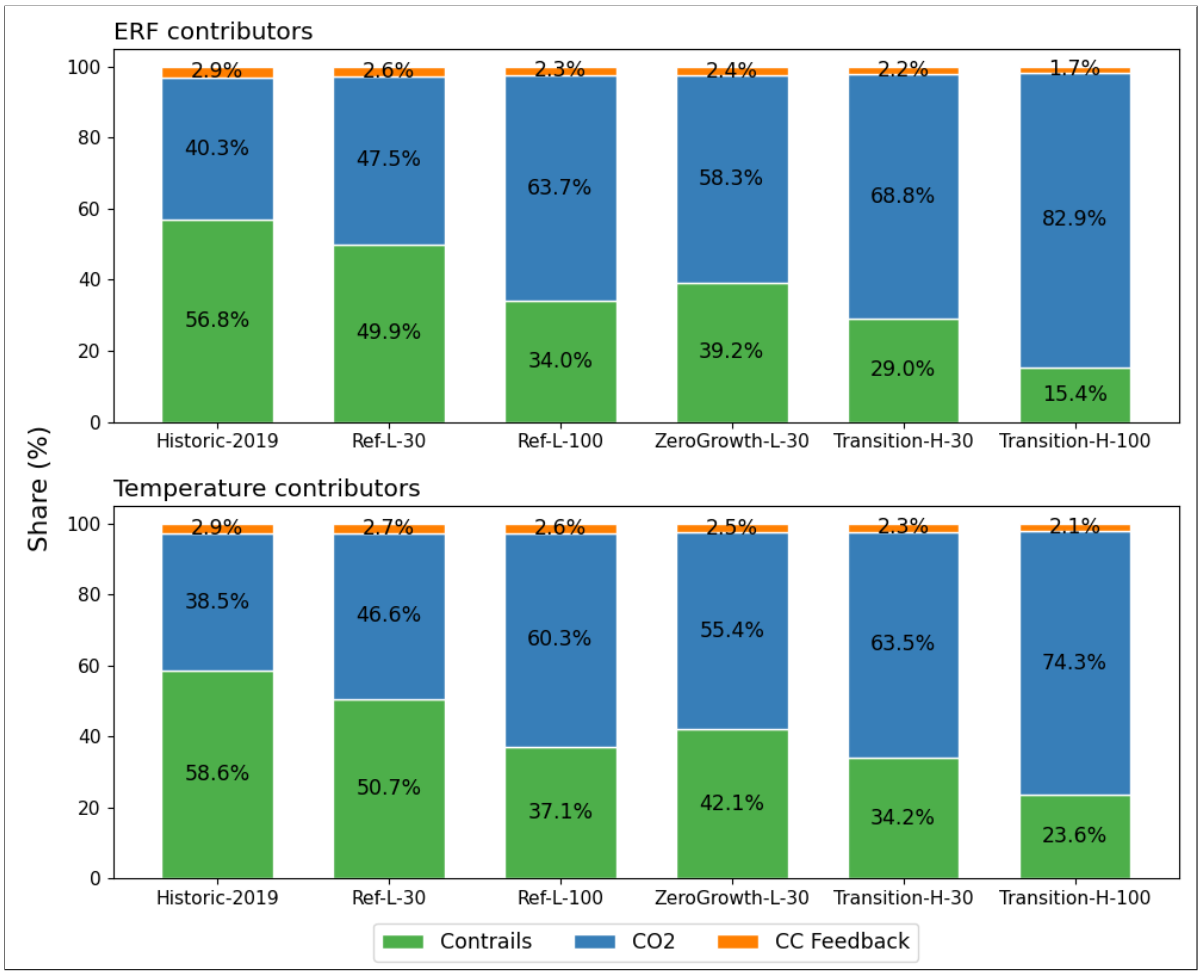


**Figure 5.4:** The above compartment displays the contribution of each forcer to the total ERF in 2050, except for the first bar; Historic-2019 which displays the contributions in 2019 before scenario-specific parameters take effect. The bottom compartment shows the forcers contribution to the temperature response in the same way.

By comparing the two compartments it is possible to see the inertia of the climate, as temperature change attributed to contrails constitute a larger share compared to the ERF of contrails by 2050. Across the board, carbon cycle feedback composes a comparatively small fraction of forcing and warming. Viewing the pre-pandemic percentages in 2019 it is evident that contrails make up a significant part of the climate impact associated with aviation, almost up to 60%. Furthermore, comparing

the distribution in 2019 to the other scenarios, the consequence of SAF-compromised fuel blends becomes clear, as the relative share of contrail warming decreases. In the Transition$^{H}_{100}$ scenario, contrail induced forcing makes up 23.6% of the total warming effect of 0.096 mK, this can be compared to the Transition$^{H}_{30}$ scenario for which contrails instead constitute 34.2% of the total warming effect of 0.121 mK. As previously established, a very similar outcome as that of Transition$^{H}_{30}$ is found in the Ref$^{L}_{100}$ scenario, which has a final warming effect of 0.120 mK. This can also be seen in the breakdown of the individual climate forcers. ZeroGrowth$^{L}_{30}$ is the scenario which falls closest in the middle between the edge cases, with a final warming effect of 0.149 mK. Although appearing in the middle, the share of contrail warming is much closer to that of Ref$^{L}_{30}$ than Transition$^{H}_{100}$. This partly exhibits the effect of an increased share of SAF, which due to the non-linearity becomes more impactful for higher percentages when it comes to reducing contrail ERF.

## 5.4 Parametrization of SAF to contrails ERF

Figure 5.5 shows the relationship between the share of SAF in the overall jet fuel composition and the reduced fraction of ERF, in relation to 100% fossil jet fuel-based contrail ERF. The relationship which was derived in this study is depicted by the solid green line and is compared to the respective relationships which has been established in studies by Klöwer et al. (2021) and Grewe et al. (2021). Although being highly similar, the relationship presented by Grewe et al. (2021) initially assumes a slower reduction in ERF for smaller shares of SAF. It is also noticeable how the expression developed in this thesis does not eliminate contrail ERF entirely after reaching a 100% SAF-based jet fuel, as opposed to the two other studies.

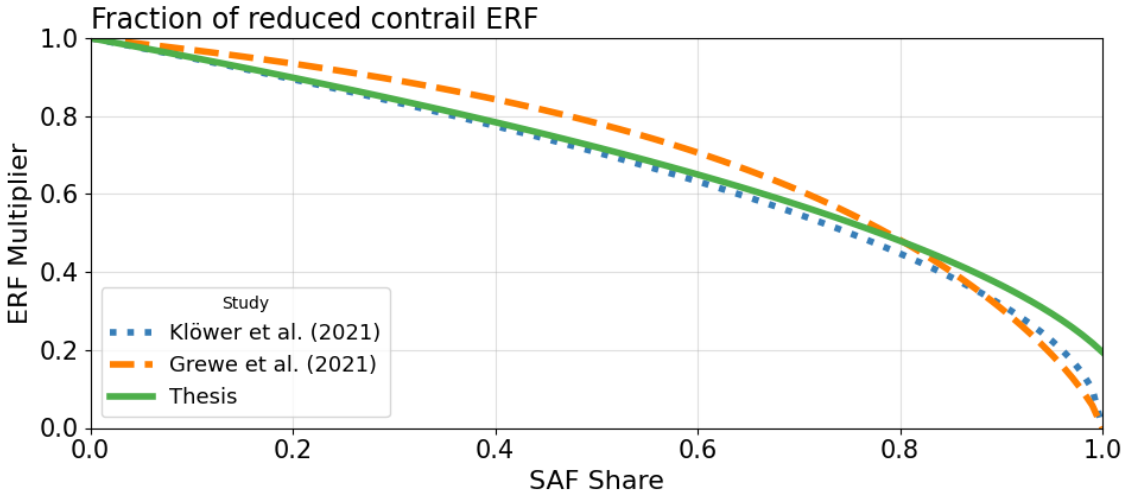


**Figure 5.5:** The reduced fraction of contrails ERF in relation to current emissions, as a function of the share of SAF in the overall jet fuel composition. The relationship developed in the study is compared to the ones by Klöwer et al. (2021) and Grewe et al. (2021).

However, Grewe et al. (2021) states that their expression is not to be used for SAF shares exceeding 90% of the total jet fuel volume.

All of the three expressions in the figure above are in part based on the reduced fraction of ice crystal numbers to ERF relationship presented by Burkhardt et al. (2018). Where both the studies by Klöwer and Grewe implement a linear scaling between the share of SAF and subsequent reduction in particle emissions upon fuel combustion, the expression which was derived in this thesis presents a different approach. It instead proposes to subtract the reduced number of ice crystals from current ice crystal numbers of a 100% fossil-based reference fuel, as used in blended fuels. Where the reduced number of ice crystals are derived from the share of SAF in the overall jet fuel blend and the succeeding linear reduction in fuel aromatic content. The given outcome following use of this expression is further interpreted in the Discussion chapter.

# 6 | Discussion

## 6.1 On policy decisions & SAF

The results indicate that the adoption of 100% SAF serves as a more potent policy instrument, regardless of continued fuel bunkering growth, as opposed to directly decreasing bunkering volumes or increasing energy efficiency, but still keeping the reduction obligation quota static at its current stipulation of a 27% greenhouse gas reduction. Halting the growth of fuel bunkering while introducing higher shares of sustainable aviation fuels would give the most significant reduction in terms of emissions and climate warming.

Compared to drastically decreasing the total fuel bunkering volumes, the implementation of pure SAF jet fuel blends however comes with its own challenges. Current regulations limit jet fuel blends to an upper ceiling of 50% drop-in fuel (SOU 2019) as the presence of aromatics still is required for present aircraft engine designs. It is however possible to design engines with seals that are not dependent on the aromatic content in order not to swell (Faber et al. 2022). But due to large inertia in the aviation industry, implementation of such engine specifications could potentially take multiple decennia. Based on the time needed to introduce new aircraft, which includes development, legislation, testing and production, such a transformation could take 45-65 years if an entire aircraft fleet were to be replaced (Åkerman et al. 2021). A case could be made for a faster implementation where only engines could be concerned but it is difficult to determine an exact time frame. It is on the other hand possible to implement 100% SAF blends with added aromatics (SOU 2019). While the side effect of sooting still would remain, albeit decreased, further reductions would still be made in terms of emitted $CO_2$ both from an end-of-pipe and a life cycle perspective because of the sustainability criteria required for producing SAF (SOU 2019).

Another point of contention is the supposed cost and availability of SAF. The price of kerosene jet fuel is highly dependent on the oil price, which saw a cost of approximately 6 SEK per litre during 2018. Comparing that to the price of bio-based SAF there is a large discrepancy, as the cost is estimated to be around 18 SEK per litre fuel in 2021 and prospectively estimated to decrease to around 12 SEK/litre by 2030 (SOU 2019). Costs can likely be reduced due to upscaling of fuel production, whereas upscaling would be likely to decrease $CO_2$ emissions related to jet fuel production as well. However, reliant on available supply and demand, produc-

ers of biofuels might be more inclined to produce fuel for road traffic rather than aviation, depending on where the most money can be made, this because currently available raw material is limited (Faber et al. 2022). Although jet fuel costs of SAF are higher, some studies demonstrate that there is a certain willingness by customers to pay more if flights were to be more climate-friendly (SOU 2019). The time which it would take to update aircraft fleets to be capable of flying with 100% SAF, containing zero aromatic content, would suggest that a combination of policy instruments are necessary in order to reduce climate warming of aviation at a faster pace. This would also be the case if biofuel availability was to be an obstacle. An interesting pathway for future studies would be to investigate the associated cost of the different scenarios, to get an idea of the range in which the feasibility of the scenarios lie. Many alternatives have been presented when it comes to reducing the aviation-related emissions, however the viability and cost-effectiveness of different solutions would have to be researched in order to provide an appropriate foundation for decision makers.

Parallels can be drawn to the proposed Fit for 55 package, which encompasses achieving strict EU climate targets by 2030 and an overall reduction of 55% net-emissions compared to 1990. A recent paper by Eurocontrol (2022) relates these cutbacks to aviation and the potential implication for policy implementations, which is described as being very reliant on market based measures. Similarly, in the paper SAF is described as being 2-6 times more costly as to kerosene jet fuel. Suggestively these high costs could be combated through taxation targeted towards kerosene jet fuel, and/or increasing the obligations of the EU emissions trading system, ultimately making the cost of SAF relatively low. The paper by Eurocontrol (2022) also mentions measures taken within the industry for reducing emissions, in this case relating to efficiency gains in fuel consumption and improvements to the aircraft designs. These improvements could work to bringing down the costs related to implementation of SAF.

### 6.1.1 Warming effect in relation to car emissions

To put the potential warming effect of Swedish jet fuel bunkering into perspective, Figure 6.1 compares the results of the historic warming effect of bunkered jet fuel, to that of end-of-pipe car emissions in Sweden when run through the climate model. In addition, a bare comparison between the two is given for 2050 if the temperature development was to follow the lines of officially set out climate targets related to reducing the amount of emissions up until this point. For the aviation industry this development is estimated to follow the $\text{Ref}_{30}^{L}$ scenario. In the case of passenger car-related emissions, the net amount of emissions are assumed to have been lowered 70% by 2030, as compared to 2010, and to have been further decreased to net zero emissions by 2045 (Naturvårdsverket n.d.[b]; Naturvårdsverket n.d.[c]). While the figure shows that car traffic in Sweden contributes to a larger warming effect, it is evident that aviation emissions related to bunkering produces a non-negligible response. With unchanged climate targets, the difference between aviation-related warming and the warming effect of passenger cars becomes gradually smaller. Emis-

sions related to aviation might become an even larger topic for discussion in the future due to the relative increase of warming from this mode of transport, given a development which reaches the set out climate targets.

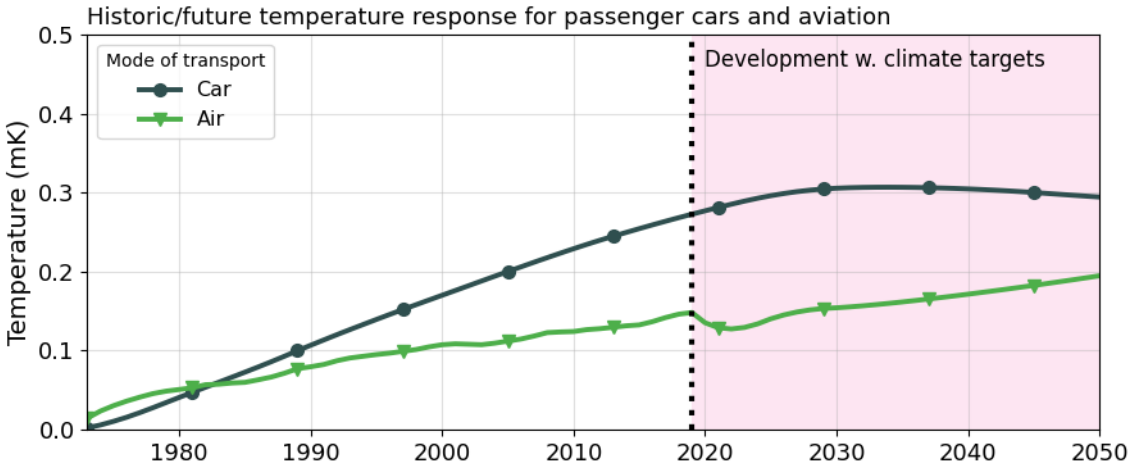


**Figure 6.1:** Global warming of fuel use pertaining to bunkering in Sweden for both cars and aircraft. In the shaded area the development of global warming follows a projection of a continued emission change in line with current climate targets (note that this composes a net decrease in annual car emissions). Data from Energimyndigheten (2020) and SCB (2020).

## 6.2 Contrails ERF as a function of SAF

As shown in Figure 5.5, the relationship between the share of SAF and the reduced fraction of contrail ERF which was derived in the thesis, does not entirely eliminate contrail forcing for 100% SAF fuel blends, like it does for the compared expressions of Klöwer et al. (2021) and Grewe et al. (2021). The consequence of contrails not being entirely eliminated, suggestively proposes a more accurate depiction of reality. Early results of the ECLIF3 project test flights (by Airbus, DLR and others) utilising 100% SAF indicate that while particle emissions are reduced, they are not removed (Airbus 2021). While aromatics have been identified as the primary cause of soot particle formation, they are not declared to be the only source. Faber et al. (2022) state that the process of soot particle formation during jet fuel combustion is generally not very well understood. Whereas more data is needed and exact measurements from the ECLIF3 and VOLCAN tests are anticipated later during 2022, a recent study by Tran et al. (2020) however measured a 97% reduction in soot emissions compared to a reference Jet A1 fuel, when using a 100% ATJ-SPK (Alcohol-to-jet) jet fuel blend, a type of fuel which is not yet available commercially (SOU 2019). More definitive research is necessary but excluding contrail induced forcing for 100% SAF fuel blends would seemingly underestimate the total global

warming effect of aviation for such fuel compositions. To which degree though has to be further investigated.

While not excluding the radiative effect of contrails for 100% SAF fuel blends, the expression which was derived in this study is limited by being based on a specific kerosene-based blend of Jet A1 fuel, as well as a specific HEFA-SPK jet fuel blend. As presented by Voigt et al. (2021) the density of aromatic content is variable for different fuels, even those consisting only of kerosene-based jet fuel. As such, the expression should not be effectively interpreted as a general relationship for all jet fuel blends containing some percentage of SAF. Whether or not it is possible to derive such an expression is however ambiguous. The exact fuel composition of 100% commercial SAF is not well understood. It can also be questioned whether there will exist a uniform SAF standard, for which a general expression could be derived. For instance, the aromatic content in Jet A1 fuel is variable depending on the fuel supplier (Faber et al. 2022).

## 6.3 Sensitivity of results

No sensitivity analysis has been conducted for the results of the study, but it should be contemplated that quantifying a definite climate impact is ambitious at best. While Lee et al. (2021) attributed contrails to an effective radiative forcing of 57.4 $mWm^{-2}$ globally in 2018, this is with a 90% likelihood of the contrail forcing being in the range between 17-91 $mWm^{-2}$. It should therefore be considered that the results of this study could be either over- or underestimated. Furthermore, Faber et al. (2022) states that two modelling teams have investigated the change of contrail cirrus in respects to particle emissions, and these provide conflicting results. As seen, what has been applied in this study is the work by the team of Burkhardt et al. (2018), which shows up frequently in related works.

# 7 | Conclusion

Aviation contributes a substantial part to global warming and when it comes to mitigating climate change, no stone can be left unturned. The results indicate that it is possible to reduce the warming associated with Swedish fuel bunkering by a substantial amount. Furthermore, it was seen that a promising solution as to reduce emissions from aircraft is through the application of sustainable aviation fuels, which reduces both $CO_2$ emissions as well as formation of contrail cirrus.

Emissions related to bunkering of jet fuel in Sweden have historically contributed to a warming effect of 0.135 mK, up until the COVID-19 pandemic. This effect is slightly less than half of the warming effect which can be attributed to end-of-pipe car emissions in Sweden during the same time period.

It was shown in the study that the potential of SAF as a means to reduce global warming has big capability. Implementing a fully SAF-based jet fuel could for the most optimistic transition scenario reduce the global warming by up to 46-53%, compared to a development of the Swedish aviation industry which follows historic trends. Even if bunkering volumes were to follow past growth, increasing the reduction obligation quota from a share of 30% SAF to 100% by 2045, could in turn reduce the relative warming by 31-42% in 2050, depending on rate of efficiency improvements during this time period. It was shown that the main reason an increased share of SAF decreases the global warming, associated with fuel bunkering in the investigated time interval, is because of the immediate reduction in contrail formation. This was found to be the most potent short-term climate forcer investigated in the study.

Among pathways to reduce emissions from aviation, policy decisions promoting the use of SAF have a comparatively larger impact, compared to reducing bunkering volumes to the extent which was investigated in the study. This is partly due to the drastic reduction in contrail forcing stemming from the use of SAF. The same goes for improvements relating to energy efficiency gains. This was also seen to be reflected in the Fit for 55 analysis of the aviation industry, where the most significant change to reducing emissions was directed towards promoting the use of SAF.

# Bibliography


Air bp (n.d.). *Jet fuel*. URL: https://www.bp.com/en/global/air-bp/aviation-fuel/jet-fuel.html.

Airbus (2021). *This chase aircraft is tracking 100% SAF's emissions performance*. URL: https://www.airbus.com/en/newsroom/stories/2021-11-this-chase-aircraft-is-tracking-100-safs-emissions-performance (visited on 05/29/2022).

Åkerman, J., A. Kamb, J. Larsson, and J. Nässén (Oct. 2021). "Low-carbon scenarios for long-distance travel 2060". In: *Transportation Research Part D: Transport and Environment* 99, p. 103010. ISSN: 13619209. DOI: 10.1016/j.trd.2021.103010. URL: https://linkinghub.elsevier.com/retrieve/pii/S1361920921003084 (visited on 05/25/2022).

Bräuer, T., C. Voigt, D. Sauer, S. Kaufmann, V. Hahn, M. Scheibe, H. Schlager, F. Huber, P. Le Clercq, R. H. Moore, and B. E. Anderson (Nov. 2021). "Reduced ice number concentrations in contrails from low-aromatic biofuel blends". In: *Atmospheric Chemistry and Physics* 21.22, pp. 16817–16826. ISSN: 1680-7324. DOI: 10.5194/acp-21-16817-2021. URL: https://acp.copernicus.org/articles/21/16817/2021/ (visited on 02/13/2022).

Burkhardt, U., L. Bock, and A. Bier (Dec. 2018). "Mitigating the contrail cirrus climate impact by reducing aircraft soot number emissions". In: *npj Climate and Atmospheric Science* 1.1, p. 37. ISSN: 2397-3722. DOI: 10.1038/s41612-018-0046-4. URL: http://www.nature.com/articles/s41612-018-0046-4 (visited on 03/23/2022).

De Jong, S.A. (2018). *Green horizons: On the production costs, climate impact and future supply of renewable jet fuels*. OCLC: 8086916135. Utrecht University. ISBN: 978-90-8672-081-1.

Energimyndigheten (2020). *Energianvändning i transportsektorn (inrikes och utrikes) uppdelad på transportslag samt bränsleslag, 1970-*. Data retrieved from Energimyndigheten Statistikdatabas, https://pxexternal.energimyndigheten.se/pxweb/sv/?rxid=d64f7a07-90c5-418f-8cb3-ca12ba959187.

Enting, I.G. (Oct. 2007). "Laplace transform analysis of the carbon cycle". In: *Environmental Modelling & Software* 22.10, pp. 1488–1497. ISSN: 13648152. DOI: 10.1016/j.envsoft.2006.06.018. URL: https://linkinghub.elsevier.com/retrieve/pii/S1364815206002775 (visited on 05/20/2022).

Eurocontrol (2022). *EUROCONTROL publishes new Think Paper: Reducing aviation emissions by 55% by 2030*. URL: https://www.eurocontrol.int/press-release/eurocontrol-publishes-new-think-paper-reducing-aviation-emissions-55-2030 (visited on 05/31/2022).

Faber, J., J. Király, D. Lee, B. Owen, and A. O'Leary (Feb. 2022). *Potential for reducing aviation non-CO2 emissions through cleaner jet fuel*. Tech. rep. CE Delft. URL: https://cedelft.eu/wp-content/uploads/sites/2/2022/03/CE_Delft_210410_Potential_reducing_aviation_non-CO2_emissions_cleaner_jet_fuel_FINAL.pdf (visited on 04/01/2022).

Flemming, G. and I. de Lépinay (2019). *Environmental Trends in Aviation to 2050*. Tech. rep. ICAO. URL: https://www.icao.int/environmental-protection/Documents/EnvironmentalReports/2019/ENVReport2019_pg17-23.pdf (visited on 05/06/2022).

Forster, P., T. Storlvmo, K. Armour, W Collins, J.-L. Dufresne, D. Frame, D.J. Lundt, T. Mauritsen, M.D. Palmer, M. Watanabe, M. Wild, and H. Zhang (2021). "The Earth's Energy Budget, Climate Feedbacks, and Climate Sensitivity". In: *Climate Change 2021: The Physical Science Basis. Contribution of Working Group I to the Sixth Assessment Report of the Intergovernmental Panel on Climate Change*, pp. 923–1054. DOI: 10.1017/9781009157896.009. URL: https://www.ipcc.ch/report/ar6/wg1/downloads/report/IPCC_AR6_WGI_Chapter07.pdf (visited on 05/02/2022).

Gasser, T., G. P. Peters, J. Fuglestvedt, W. Collins, D. Shindell, and P. Ciais (Apr. 2017). "Accounting for the climate–carbon feedback in emission metrics". In: *Earth System Dynamics* 8.2, pp. 235–253. ISSN: 2190-4987. DOI: 10.5194/esd-8-235-2017. URL: https://esd.copernicus.org/articles/8/235/2017/ (visited on 04/25/2022).

Gierens, K., S. Matthes, and S. Rohs (Dec. 2020). "How Well Can Persistent Contrails Be Predicted?" In: *Aerospace* 7.12, p. 169. ISSN: 2226-4310. DOI: 10.3390/aerospace7120169. URL: https://www.mdpi.com/2226-4310/7/12/169 (visited on 03/22/2022).

Government of Canada (2016). *Volume correction factors—Jet A, Jet-A1, jet kerosene, turbine fuel*. URL: https://www.ic.gc.ca/eic/site/mc-mc.nsf/eng/lm04778.html (visited on 05/26/2022).

Grewe, V., A. Gangoli Rao, T. Grönstedt, C. Xisto, F. Linke, J. Melkert, J. Middel, B. Ohlenforst, S. Blakey, S. Christie, S. Matthes, and K. Dahlmann (Dec. 2021). "Evaluating the climate impact of aviation emission scenarios towards the Paris agreement including COVID-19 effects". In: *Nature Communications* 12.1, p. 3841. ISSN: 2041-1723. DOI: 10.1038/s41467-021-24091-y. URL: http://www.nature.com/articles/s41467-021-24091-y (visited on 05/16/2022).

Holladay, J., Z. Abdullah, and J. Heyne (2020). *Sustainable aviation fuel review of technical Pathways*. Tech. rep. U.S. Department of Energy. URL: https://www.energy.gov/sites/prod/files/2020/09/f78/beto-sust-aviation-fuel-sep-2020.pdf (visited on 05/01/2022).

IATA (Mar. 2022). *Air Passenger Numbers to Recover in 2024*. URL: https://www.iata.org/en/pressroom/2022-releases/2022-03-01-01/ (visited on 05/06/2022).

Jiménez-Díaz, L., A. Caballero, N. Pérez-Hernández, and A. Segura (Jan. 2017). "Microbial alkane production for jet fuel industry: motivation, state of the art and perspectives". In: *Microbial Biotechnology* 10.1, pp. 103–124. ISSN: 17517915. DOI: 10.1111/1751-7915.12423. URL: https://onlinelibrary.wiley.com/doi/10.1111/1751-7915.12423 (visited on 04/13/2022).

Johansson, D. (Sept. 2020). *Lecture notes: Climate change III – climate sensitivity, ocean heat uptake, and sea level rise.* Department of Space Earth and Environment, Chalmers University of Technology.

Joos, F., R. Roth, J. S. Fuglestvedt, G. P. Peters, I. G. Enting, W. von Bloh, V. Brovkin, E. J. Burke, M. Eby, N. R. Edwards, T. Friedrich, T. L. Frölicher, P. R. Halloran, P. B. Holden, C. Jones, T. Kleinen, F. T. Mackenzie, K. Matsumoto, M. Meinshausen, G.-K. Plattner, A. Reisinger, J. Segschneider, G. Shaffer, M. Steinacher, K. Strassmann, K. Tanaka, A. Timmermann, and A. J. Weaver (Mar. 8, 2013). "Carbon dioxide and climate impulse response functions for the computation of greenhouse gas metrics: a multi-model analysis". In: *Atmospheric Chemistry and Physics* 13.5, pp. 2793–2825. ISSN: 1680-7324. DOI: 10.5194/acp-13-2793-2013. URL: https://acp.copernicus.org/articles/13/2793/2013/ (visited on 02/07/2022).

Kamb, A. and J. Larsson (2019). "Climate footprint from Swedish residents' air travel". In: URL: https://research.chalmers.se/publication/508693/file/508693_Fulltext.pdf (visited on 05/02/2022).

Kandaramath Hari, T., Z. Yaakob, and N. N. Binitha (Feb. 2015). "Aviation biofuel from renewable resources: Routes, opportunities and challenges". In: *Renewable and Sustainable Energy Reviews* 42, pp. 1234–1244. ISSN: 13640321. DOI: 10.1016/j.rser.2014.10.095. URL: https://linkinghub.elsevier.com/retrieve/pii/S1364032114009204 (visited on 04/13/2022).

Kärcher, B. (Dec. 2018). "Formation and radiative forcing of contrail cirrus". In: *Nature Communications* 9.1, p. 1824. ISSN: 2041-1723. DOI: 10.1038/s41467-018-04068-0. URL: http://www.nature.com/articles/s41467-018-04068-0 (visited on 03/22/2022).

Klöwer, M., M. R. Allen, D. S. Lee, S. R. Proud, L. Gallagher, and A. Skowron (Oct. 2021). "Quantifying aviation's contribution to global warming". In: *Environmental Research Letters* 16.10. Publisher: IOP Publishing, p. 104027. ISSN: 1748-9326. DOI: 10.1088/1748-9326/ac286e. URL: https://doi.org/10.1088/1748-9326/ac286e (visited on 02/04/2022).

Larsson, J., J. Morfeldt, D. Johansson, J. Rootzén, C. Hult, J. Åkerman, F. Hedenus, F. Sprei, and J. Nässén (2021). *Konsumtionsbaserade scenarier för Sverige - underlag för diskussioner om nya klimatmål*. Tech. rep. Mistra Sustainable Consumption, Rapport 1:11. Göteborg: Chalmers Tekniska Högskola. URL: https://research.chalmers.se/publication/526528/file/526528_Fulltext.pdf (visited on 05/06/2022).

Lee, D.S., D.W. Fahey, A. Skowron, M.R. Allen, U. Burkhardt, Q. Chen, S.J. Doherty, S. Freeman, P.M. Forster, J. Fuglestvedt, A. Gettelman, R.R. De León, L.L. Lim, M.T. Lund, R.J. Millar, B. Owen, J.E. Penner, G. Pitari, M.J. Prather, R. Sausen, and L.J. Wilcox (Jan. 2021). "The contribution of global aviation to anthropogenic climate forcing for 2000 to 2018". In: *Atmospheric Environment* 244, p. 117834. ISSN: 13522310. DOI: 10.1016/j.atmosenv.2020.117834. URL: https://linkinghub.elsevier.com/retrieve/pii/S1352231020305689 (visited on 02/04/2022).

Mason-Delmotte, V., P. Zhai, A. Pirani, S.L. Connors, C. Péan, S. Beger, N. Cause, Y Chen, L. Goldfarb, M.I. Gomis, M. Huang, K. Leitzell, E. Lonnoy, J.B.R. Matthers, T.K. Maycock, T. Waterfield, O. Yelekci, R. Yu, and B. Zhou (2021). "IPCC, 2021: Summary for Policymakers". In: *Climate Change 2021: The Physical Science Basis. Contribution of Working Group I to the Sixth Assessment Report of the Intergovernmental Panel on Climate Change*. URL: https://www.ipcc.ch/report/ar6/wg1/downloads/report/IPCC_AR6_WGI_SPM_final.pdf (visited on 05/02/2022).

Naturvårdsverket (n.d.[a]). *Flygets klimatpåverkan*. URL: https://www.naturvardsverket.se/amnesomraden/klimatomstallningen/omraden/klimatet-och-konsumtionen/flygets-klimatpaverkan.

– (n.d.[b]). *Inrikes transporter, utsläpp av växthusgaser*. URL: https://www.naturvardsverket.se/data-och-statistik/klimat/vaxthusgaser-utslapp-fran-inrikes-transporter/.

– (n.d.[c]). *Sveriges klimatmål och klimatpolitiska ramverk*. URL: https://www.naturvardsverket.se/amnesomraden/klimatomstallningen/sveriges-klimatarbete/sveriges-klimatmal-och-klimatpolitiska-ramverk/.

Richter, S., T. Kathrotia, C. Naumann, S. Scheuermann, and U. Riedel (Jan. 2021). "Investigation of the sooting propensity of aviation fuel mixtures". In: *CEAS Aeronautical Journal* 12.1, pp. 115–123. ISSN: 1869-5582, 1869-5590. DOI: 10.1007/s13272-020-00482-7. URL: http://link.springer.com/10.1007/s13272-020-00482-7 (visited on 04/07/2022).

Sampson, B. (Nov. 1, 2021). "Airbus flies A319neo on 100% sustainable aviation fuel for first time". In: *Aerospace Testing International*. URL: https://www.aerospacetestinginternational.com/news/flight-testing/airbus-flies-a319neo-on-100-sustainable-aviation-fuel-for-first-time.html (visited on 05/02/2022).

Sausen, R. and U. Schumann (2000). "Estimates of the Climate Response to Aircraft CO2 and NOx-Emission Scenarios". In: *Climatic Change* 44.1, pp. 27–58. ISSN: 01650009. DOI: 10.1023/A:1005579306109. URL: http://link.springer.com/10.1023/A:1005579306109 (visited on 04/13/2022).

SCB (2020). *Utsläpp av växthusgaser från inrikes transporter efter växthusgas, transportslag, bränsleslag och år*. Data retrieved from SCB Statistikdatabasen, https://www.statistikdatabasen.scb.se/pxweb/sv/ssd/START__MI__MI0107/MI0107InTranspN/.

Schumann, U. (1996). "On conditions for contrail formation from aircraft exhausts". In: *Meteorol. Zeitschrift* 5, pp. 4–23. URL: https://elib.dlr.de/32128/1/mz-96.pdf (visited on 03/22/2022).

– (May 2005). "Formation, properties and climatic effects of contrails". In: *Comptes Rendus Physique* 6.4, pp. 549–565. ISSN: 16310705. DOI: 10.1016/j.crhy.2005.05.002. URL: https://linkinghub.elsevier.com/retrieve/pii/S1631070505000563 (visited on 03/22/2022).

Smith, C., Z.R.J. Nicholls, K. Armour, W. Collins, P. Forster, M. Meinshausen, M.D. Palmer, and M. Watanabe (2021). "The Earth's Energy Budget, Climate Feedbacks, and Climate Sensitivity Supplementary Material". In: *Climate Change 2021: The Physical Science Basis Contribution of Working Group I to the Sixth Assessment Report of the Intergovernmental Panel on Climate Change*. URL: https://www.ipcc.ch/ (visited on 04/19/2022).

SOU, ed. (2019). *Biojet för flyget*. Statens offentliga utredningar 2019:11. Stockholm: Norstedts Juridik. 326 pp. ISBN: 978-91-38-24907-9.

SOU, ed. (2022). *Sveriges globala klimatavtryck*. Statens offentliga utredningar 2019:11. Stockholm: Norstedts Juridik. 326 pp. ISBN: 978-91-525-0355-3.

Sveriges Riksdag (2021). *Jet fuel*. URL: https://www.riksdagen.se/sv/dokument-lagar/dokument/proposition/reduktionsplikt-for-flygfotogen_H803135/html (visited on 05/26/2022).

Terrenoire, E., D. A. Hauglustaine, T. Gasser, and O. Penanhoat (Aug. 1, 2019). "The contribution of carbon dioxide emissions from the aviation sector to future climate change". In: *Environmental Research Letters* 14.8, p. 084019. ISSN: 1748-9326. DOI: 10.1088/1748-9326/ab3086. URL: https://iopscience.iop.org/article/10.1088/1748-9326/ab3086 (visited on 05/06/2022).

Toru, H. (2021). *Effects of Novel Coronavirus (COVID-19) on Civil Aviation: Economic Impact Analysis*. ICAO, https://www.icao.int/sustainability/Documents/COVID-19/ICAO%20COVID%202021%2009%2022%20Economic%20Impact%20TH%20Toru.pdf.

Tran, S., A. Brown, and J. S. Olfert (June 2020). "Comparison of Particle Number Emissions from In-Flight Aircraft Fueled with Jet A1, JP-5 and an Alcohol-to-Jet Fuel Blend". In: *Energy & Fuels* 34.6, pp. 7218–7222. ISSN: 0887-0624, 1520-5029. DOI: 10.1021/acs.energyfuels.0c00260. URL: https://pubs.acs.org/doi/10.1021/acs.energyfuels.0c00260 (visited on 05/29/2022).

Transportstyrelsen (Apr. 2021). *Passagerarprognos 2021–2027*. Tech. rep. Sjö- och luftfartsavdelningen, enheten för hållbar utveckling. URL: https://www.transportstyrelsen.se/globalassets/global/publikationer/luftfart/prognos-slutlig_var-2021.pdf (visited on 05/07/2022).

Unterstrasser, S. (Feb. 2016). "Properties of young contrails – a parametrisation based on large-eddy simulations". In: *Atmospheric Chemistry and Physics* 16.4, pp. 2059–2082. ISSN: 1680-7324. DOI: 10.5194/acp-16-2059-2016. URL: https://acp.copernicus.org/articles/16/2059/2016/ (visited on 04/26/2022).

Voigt, C., J. Kleine, D. Sauer, R. H. Moore, T. Bräuer, P. Le Clercq, S. Kaufmann, M. Scheibe, T. Jurkat-Witschas, M. Aigner, U. Bauder, Y. Boose, S. Borrmann, E. Crosbie, G. S. Diskin, J. Di Gangi, V. Hahn, C. Heckl, F. Huber, J. B. Nowak, M. Rapp, B. Rauch, C. Robinson, T. Schripp, M. Shook, E. Winstead, L. Ziemba, H. Schlager, and B. E. Anderson (Dec. 2021). "Cleaner burning aviation fuels can reduce contrail cloudiness". In: *Communications Earth & Environment* 2.1, p. 114. ISSN: 2662-4435. DOI: 10.1038/s43247-021-00174-y. URL: http://www.nature.com/articles/s43247-021-00174-y (visited on 02/13/2022).

Xie, P. and G. K. Vallis (Feb. 2012). "The passive and active nature of ocean heat uptake in idealized climate change experiments". In: *Climate Dynamics* 38.3, pp. 667–684. ISSN: 0930-7575, 1432-0894. DOI: 10.1007/s00382-011-1063-8.

URL: http://link.springer.com/10.1007/s00382-011-1063-8 (visited on 05/05/2022).

**DEPARTMENT OF SOME SUBJECT OR TECHNOLOGY**
**CHALMERS UNIVERSITY OF TECHNOLOGY**
Gothenburg, Sweden
www.chalmers.se


CHALMERS
UNIVERSITY OF TECHNOLOGY